ANALYSIS OF MAGNETIC FLUX, DYNAMIC VISCOCITY AND YIELD STRESS DISTRIBUTION IN MR DAMPER

A PROJECT REPORT

submitted by

ADHIL MOHAMMED A

TKM20MECI01

to

the APJ Abdul Kalam Technological University

in partial fulfillment of the requirements for the award of the Degree

of

Master of Technology

In

Computer Integrated Manufacturing

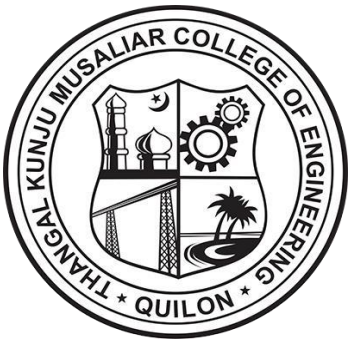

Department of Mechanical Engineering

TKM College of Engineering

Kollam

SEPTEMBER 2022

DECLARATION

I, Adhil Mohammed A, hereby declare that the project report "Analysis of magnetic flux, dynamic viscosity and yield stress distribution in MR damper", submitted for partial fulfillment of the requirements for the award of degree of Master of Technology ofthe APJ Abdul Kalam Technological University, Kerala is a bonafide work done by me under supervision of Rizwan Rasheed, Assistant Professor, Department of Mechanical Engineering, TKM College of Engineering, Kollam. This submission represents my ideas in my own words and where ideas or words of others have been included, I have adequately and accurately cited and referenced the original sources. I also declare that I have adhered to ethics of academic honesty and integrity and have not misrepresented or fabricated any data or idea or fact or source in my submission. I understand that any violation of the above will be a cause for disciplinary action by the institute and/or the University and can also evoke penal action from the sources which have thus not been properly cited or from whom proper permission has not been obtained. This report has not been previously formed the basis for the award of any degree, diploma or similar title of any other University.

Kollam

Date: 12/09/2022 Adhil Mohammed A

DEPARTMENT OF MECHANICAL ENGINEERING
TKM COLLEGE OF ENGINEERING, KOLLAM

CERTIFICATE

This is to certify that the report entitled **"ANALYSIS OF MAGNETIC FLUX, DYNAMIC VISCOCITY AND YIELD STRESS DISTRIBUTION IN MR DAMPER"** submitted by **ADHIL MOHAMMED A, TKM20MECI01** to the APJ Abdul Kalam Technological University in partial fulfillment of the requirements for the award of the Degree of Master of Technology in Computer Integrated Manufacturing, Department of Mechanical Engineering, is a bonafide record of the project work carried out by him/her under my/our guidance and supervision. This report in any form has not been submitted to any other University or Institute for any purpose.

Supervisor : **Rizwan Rasheed**
Assistant Professor
Dept. of Mechanical Engineering
TKM college of Engineering, Kollam

PG Coordinator : **Kannan. S**
Assistant Professor
Dept. of Mechanical Engineering
TKM College of Engineering, Kollam

Dr. P.N. Dileep
Head of the department
Department of Mechanical Engineering
TKM College of Engineering, Kollam

ACKNOWLEDGEMENT

First of all, I am indebted to the **GOD ALMIGHTY** for giving me an opportunity to excel in my efforts to complete this project on time.

I am extremely grateful to **Dr. T A SHAHUL HAMEED**, Principal, TKM college of Engineering and **Dr. P.N. DILEEP**, Head of the Department, Department of Mechanical Engineering, for providing all required resources for successful completion of my project.

I am greatly obliged to my internal supervisor **RIZWAN RASHEED**, Assistant professor, Department of Mechanical Engineering, **ASHOK**, Phd scholar, Department of Mechanical Engineering for their encouragement, guidance and support.

My heartfelt gratitude to **Prof. KANNAN S.**, PG coordinator, Department of CIM & **Prof. FAIZAL N. S.**, Assistant professor, Department of CIM for their valuable suggestions and guidance in the preparation of the project presentation and report.

I express my thanks to all Faculties and Technical staffs, Department of Mechanical Engineering, and all staff members and friends for all help and coordination extended in bringing out this project successfully in time.

I will be failing in duty if I do not acknowledge with grateful thanks to the authors of the references and other literatures referred to in this project.

Last but not the least, I am very much thankful to my parents who guided me in every steps which I took.

Place: KOLLAM **ADHIL MOHAMMED A**

Date: 12/09/2022

ABSTRACT

Magnetorheological materials are smart materials where its rheological characteristics can be quickly changed by the introduction of a magnetic field. The electromagnet and a piston submerged in an MR fluid make up the MR damper. The MR fluid solidifies as Electromagnet is subjected to current, and its yield stress changes in reaction the magnetic field that is being used. Therefore, the magnetic field generation is a significant MR damper phenomenon. In this work, the magnetic field generated in the damper and dynamic viscosity was analyzed for the change in coil numbers and MR fluid gap utilizing finite element method using COMSOL Multiphysics. A 2D axisymmetric, quasi-static model was created utilizing auxiliary sweep study by changing current from 1.5–4 A and the number of coils 300,400,500 and 600 effects on the magnetic flux density, yield stress, and dynamic viscosity change caused by externally applied current in the fluid flow gap of the MR fluid were assessed and for the fluid flow gap of 1mm,1.5mm,2mm with 400 coil turns. The inference obtained after the analysis of results are as the current is increased the magnetic flux density is also increasing in the MR fluid and as the magnetic flux intensity increases the yield stress and dynamic viscosity also increases with the current. When the number of turns in coil increases the magnetic flux density also increases proportionally and there by yield stress and dynamic viscosity also increases. When the gap between piston and cylinder increases the magnetic flux density is decreased so there by a decrease in yield stress and dynamic viscosity is observed.

Keywords: magnetorheological material, auxiliary sweep, magnetic flux intensity, dynamic viscosity, yield stress

CONTENTS

LIST OF TABLES

LIST OF FIGURES

ABBREVIATIONS

MRF	Magnetorheological Fluid
MRD	Magnetorheological Damper
CFD	Computational Fluid Dynamics
MF	Magnetic Field

NOTATIONS

B	Magnetic flux density
H	Magnetic field
J	Current density
D	Electric displacement field
m	Model parameter

Greek Symbols

η	dynamic viscosity
η_0	zero field viscosity
$\tau_y(B)$	yield stress
$\dot{\gamma}$	shear rate

CHAPTER 1

INTRODUCTION

The MR damper is an energy absorber that performs effectively due to the rheological characteristics of the MR fluid. A magnetic field applied externally can change the rheological properties of a magnetorheological fluid, is a type of smart fluid. This smart material is made composed of tiny, magnetizable particles suspended in a carrier fluid. Carrier fluids are generally silicone oil or any other mineral oils. At zero magnetic field, MR fluid behaves like a Newtonian fluid. The MR fluid becomes a viscoelastic solid where it is subjected to a magnetic field due to an increase in viscosity. Due to that the yield stress can be modified by varying the magnetic field's intensity. Its importance lies in the MR fluid's potential to transfer the force that can be controlled by magnetic force, opening up a diverse array of potential applications for leverage.

A semi-actively regulated intelligent vibration dampening system is called a magnetorheological damper (MRD). It is a smart device because of the internal magnetorheological fluid's quick, continuous, and reversible rheological characteristics. Vehicle vibration and control have been the focus of the majority of MRD studies. MRD has recently been applied to the area of robotics. For example, research indicates that MRD is utilized in medical equipment for rehabilitation. MRD has ability to alter the damping capacity (as determined by the force for damping) in mean time to adapt alterations to the environment, as opposed to standard gas damper. This enhances the robot's controllability, stability, resilience, and robustness [1,2]. In the MR damper the resistance of the microparticle chains causes the fluid to shows an irregular yield stress when flow occurs perpendicular to magnetic flux lines. As a result, the fluid behaves like a Bingham plastic when a magnetic field is applied to the fluid gap that has some flux lines due to an electromagnetic circuit [3].

MR dampers is used in a many of vibrational control applications, including those for civil structures, railroad trains, and automobiles.

Acura MDX, Audi TT and R8, BMWs, Buick Lucerne, Cadillac DTS, Cadillac XLR, Cadillac SRX, Cadillac STS, Chevrolet Corvette, Ferrari 599GTB, and other vehicles employ this magnetorheological shock absorber.

This system's applications are not restricted to the automotive industry alone; they can also be employed in contemporary earthquake-resistant building construction and gun recoil.

Benefits of MR dampers include lower manufacturing costs, rapid response (change in viscosity occurs in a matter of milliseconds), simplicity of construction, low power consumption, and superior vibration absorption over passive devices. The size of the particles, the carrier fluid's characteristics, stabilizing agent and additives, the applied magnetic field, temperature, the concentration and density of the particles, etc. all affect the rheological characteristics of the MR fluid. It is essential to be aware of the magnetic characteristics of MR fluid when constructing MR fluid devices. Electric coils cause a magnetic flux density in an MR damper that is directly proportional to the applied field. MR fluids are resistant to environmental contaminants and are not susceptible to contaminants that are present both during production and use. where the presence of impurities, particularly water or moisture, has a significant impact on performance [4]

Recent research has concentrated on the MR damper's finite element analysis to determine magnetic flux density and optimize the geometry. Some studies focused on analysis of various structural parameters in MR damper. The analysis tool used for studies are mostly ANSYS and COMSOL Multiphysics software packages. For the proposed work COMSOL Multiphysics software is used for the analysis. To achieve an optimized design for an MR damper there is a need for a simulation system for an MR damper. This initial simulation can be used to validate the MR

damper optimized parameters. The studies for sustainable MR fluids were in progress so this initial simulation and analysis can be use for comparing the performance of the MR damper with a newly developed MR fluid. For this project work, the magnetic field generated in the damper and dynamic viscosity is analyzed for the change in coil numbers and MR fluid gap by using finite element method using COMSOL Multiphysics software.

CHAPTER 2

LITERATURE REVIEW

To investigate the effects of the current, damping gap, piston core radius, and flange length on the MRD's damping properties, Parlak et al. did a unidirectional coupling simulation analysis of MRD [5].

An MR damper of 15 tonne was designed, manufactured, and put into use in detail by Alan Sternberg et al. Using the ANSYS platform, he created a FEM 3D model where he solves the magnetic field and fluid dynamics using the Maxwell equations and the Navier-Strokes equation, respectively.

The small difference brought on by fluid compressibility was consistent with the experimental and analytical results [6].

Finite elements have been suggested by Zhang et al as a way to enhance the magnetic design of an MR damper [7].

With the aid of the FEMM programme, Izyan Iryani Mohd Yazid et al. performed an electromagnetic simulation and design of a combined MR damper model. The simulation findings were utilized to build the combined mode MR damper and afterwards used to compare the joined mode MR damper's performance to that of the single mode MR damper [8].

A comparison study was used to propose an optimization strategy by Khan et al. Simulated and studied were the damping forces of the MRD with nine different coils and various piston heads. They discovered that when the piston head is altered in the shape of rounded corners, the piston head may deliver a stronger damping force [9].

On the basis of a theoretical analysis of the magnetic circuit, Yang et al. created a MR damper with three coil and a finite element model.

Simulation was used to found out the magnetic field strength in the damping gap under various currents and coil turns [10].

A MR damper with a novel structure and controlled internal pressure was introduced by Golinelli et al. Software using finite elements was used to simulate the magnetic field of the damper. In combination with the experimental findings, it was demonstrated that the minimum and maximum damping force errors between the simulation and experiment were 8.2% and 15%, respectively [11].

S. K. Mangal et al. created a FEM model for an MR damper and used a ANSYS workstation to analyze it as an axisymmetric model and for the evaluation the magnetic geometry flux produced by the MR damper. Future MR damper designs can be based on the results to achieve the desired damping force [12].

The shape of the piston, the MR fluid gap, the air gap, and the thickness of the damper's housing were all taken into account by Ferdaus et al. while creating a 2-D axi-symmetric and 3D model of an MR damper [13].

The magneto-static study of the MR Damper was carried out by Hemanth K. et al. using ANSYS software. After 0.7A of input current, the fluid reaches saturation, which can be seen in the Force v/s Velocity graph. From this, it can be deduced that semi-active suspension outperforms passive suspension in the simulation [14].

For the creation magnetic flux density in an MR damper for medical orthoses, Case et al. first performed a Multiphysics analysis of the device using COMSOL Multiphysics [15].

Guoliang Hu et al. analyze the MR damper's dynamic performance, stress distribution, static magnetic field properties, and dynamic flow field properties under the influence of multiphysics coupling [16].

Koray Özsoy et al. studied Continuum mechanics has been used to comprehensively analyse the behavior of MR fluid. For an electromagnetic field-based continuous medium, the relevant balance equations have been written [17].

Hongzhan Lv et al. a methodical approach to the optimum MRD design for increased damping capacity and dynamic adaptability when carrying out its damping function. In order to model and simulate the MRD, the compressibility of the MR fluid is taken into account. The contributions of the parameters that determine the fluid's characteristics and the MRD's structure to dynamic adjustability and damping capacity are thoroughly investigated. The dynamically changeable coefficient and the damping force are optimized using the response surface method to configure the parameters in a more useful manner [18].

Raju Ahamed et al. conducted study for car suspension systems, a mono tube MR damper type with energy generation has been created. The Solid Works electromagnetic simulator (EMS) is used to create a 3D model of the generation of energy MR damper, which is then thoroughly examined using the finite element method [19].

W.A. Bullough et al. provide information on what can currently be accomplished to direct the pre-prototyping stage of the design of smart fluid devices and demonstrate the validity of the numerous examples used to support the theme [20].

Zekeriya Parlak et al. a method of design optimization that was used to achieve an MR damper's maximum magnetic flux density and target damper force has been given. To determine the best value for design parameters, finite element methods, electromagnetic analyses of magnetic fields,

and CFD analyses of MR flows has been applied. The novel method, that uses the magnetic field and MR flow together, has determined the ideal design parameters [21].

S. Vivekananda Sharma et al. done the study on the Finite Element for a locally produced, down-scaled MR Damper. The magnetic flux produced by an FEA can be utilized to determine the magnetic resonance damper's damping force. The size of the prototype MR damper, the magnetic circuit's geometry, the characteristics of the MR fluid, and the material employed are all covered in this study. The 3-D model created in Solid works is loaded into the magnetostatic analysis program COMSOL Multiphysics with various current inputs and coil turn changes [22].

2.1 PROBLEM STATEMENT

To achieve an optimized design for an MR damper there is a need for a simulation system for an MR damper. This initial simulation can be used to validate the MR damper optimized parameters. The studies for sustainable MR fluids were in progress, in this MR fluid by modifying oil like cooking oil is used which has not much effect on the environment unlike the silicone oil used in the most MR fluid, so this initial simulation and analysis can be used for comparing the performance of the MR damper with a newly developed MR fluid.

2.2 SCOPE OF STUDY

Construction of MR damper and testing of MR dampers are complex compared to the conventional damper. The cost involved in construction and developing MR Damper a control system is high. For constructing an MR damper which have high efficiency and effectiveness with in a cost-effective way is to done a simulation and analysis for different criteria and to optimize the damper with the analysis is to be done. A validated model can also be used to compare the performance and different parameters like magnetic flux density, yield stress, dynamic viscosity, pressure distribution and velocity distribution of different kind of MR fluids.

2.3 OBJECTIVES

The following are the objective of this study.

- Geometric Modelling of an MR Damper.
- Selection of appropriate materials for MR Damper and selecting suitable MR Fluid for simulation.
- Selection of suitable physics for Multiphysics simulation.
- Selection of coil turns number and MR gap for fluid flow for the simulation.
- Selection of suitable meshing parameters.
- Analysis of MR Damper Magnetic Flux, dynamic viscosity, yield stress distribution using COMSOL Multiphysics software.

CHAPTER 3

METHODOLOGY

To begin the simulation the materials, need to be selected. Proper materials are identified from the research publications done in the past on MR damper. The parameters for the geometry were selected in a similar way and after the selection of geometric parameters the geometry was modelled in the COMSOL Multiphysics software and the appropriate materials were added to the geometry. Identification of physics for study and the appropriate physics is added in the software interface and after loading the geometry to the software appropriate boundary conditions are given. The next step involves in creating the mesh and adding study with auxiliary sweep for different currents. Analysis of results is done after completing study.

3.1 GEOMETRIC MODELLING

A typical MR damper is shown in Figure 3.1 and it contains the piston, cylinder, floating piston, floating piston rod, lifting lug, and more parts. The piston has a multiturn coil within. Utilizing the high-pressure nitrogen compensation chamber, the floating piston is adjusted to account for the volume shift brought on by the piston rod's entry and exit.

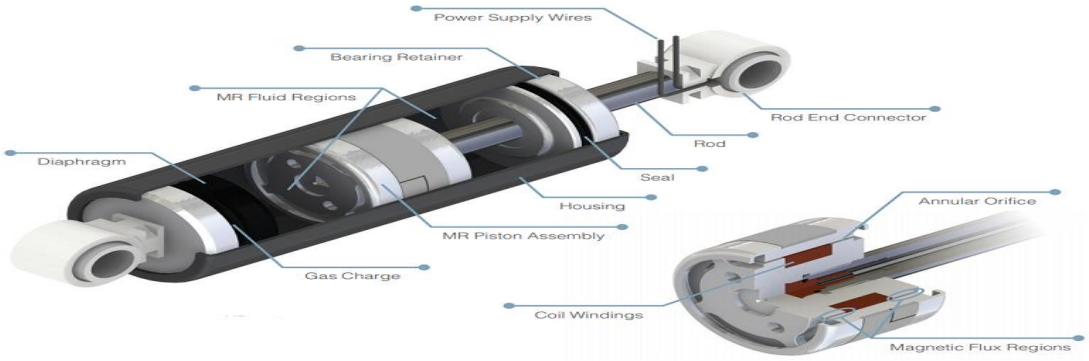

Fig.3.1 A typical MR damper (LORDS CORP)

The damping gap, or small space in between a piston and cylinder, is passed by the magnetic flux produced by the excitation coil. This space is present in the piston's center and both ends. The damper gap allows the magnetic flux to enter the cylinder while the damper gap on the opposite side allows it to exit. A closed magnetic circuit is created when the magnetic flux eventually returns to the yoke. The damping gap's MR fluid's viscosity and damping force are both affected by the magnetic field that is being provided. During this time, the MR fluid's yield stress rises the viscosity of the MR fluid rises as the current increases., and the piston is moving. The damping force of the MRD can be changed as a result.

A 2-D Axisymmetric model was chosen for modelling the damper for reducing the computational cost. The area chosen for modelling are the area of piston, cylinder, coil and MR fluid interaction occurs. An air envelope is created around the model for the magnetic insulation region. Fig 3.2 shows the modelled geometry. Table 3.1 shows the design data of the proposed MR damper.

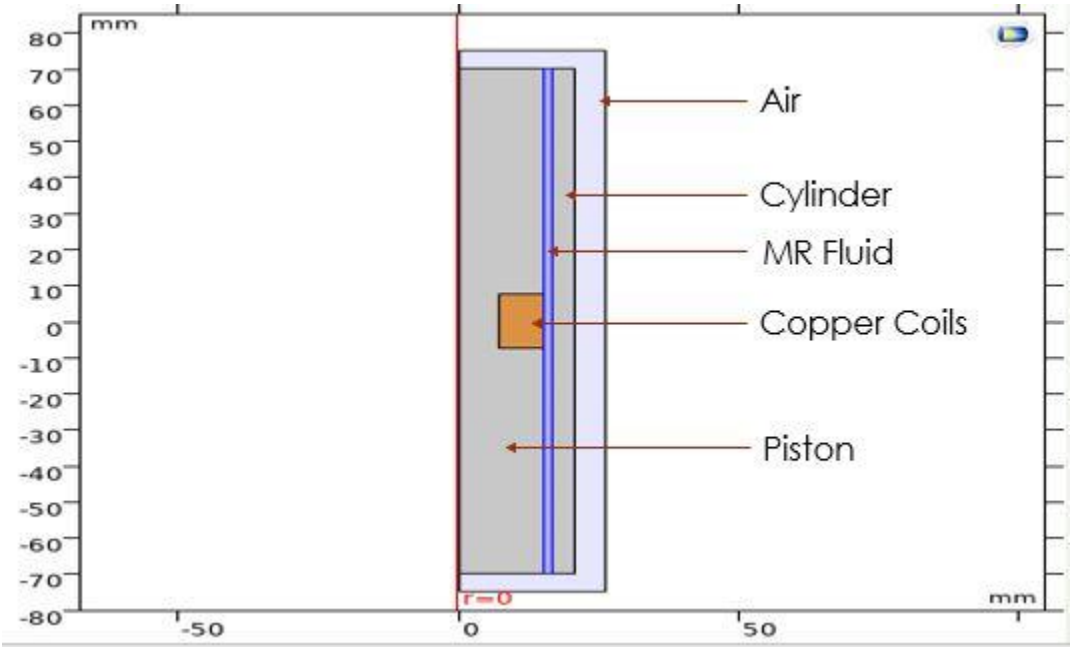

Fig.3.2 Modelled geometry

Table 3.1 Design parameters

Main Structural Parameters	**Values**
The thickness of the cylinder h	4 mm
Coil width	8 mm
Piston diameter D	30 mm
Damping gap g	1 mm
Height of cylinder	140 mm
Coil height	15 mm
Air width	26 mm
Air height	150 mm
current I	1.5 A, 2 A, 2.5 A, 3 A,3.5 A,4 A

3.2 MATERIAL SELECTION

The MRF 132DG is selected as an MR fluid for the analysis, by reviewing different research papers. The MRF 132DG is selected because of the availability of data regarding the MRF 132DG and its also widely used in MR dampers for automobiles and its wide operating temperature. The data for MRF 132DG is obtained from LORDS CORPORATION data sheet. The material for the Piston and cylinder is low carbon steel AISI 1018 which properties are readily available in COMSOL. Figure 3.3 and 3.4 shows B H curve and shear stress vs shear rate and Figure 3.5 shows the B H curve for the AISI 1018 steel. Relative permeability of MRF 132DG and AISI 1018 steel is 5.5 and 1600 respectively

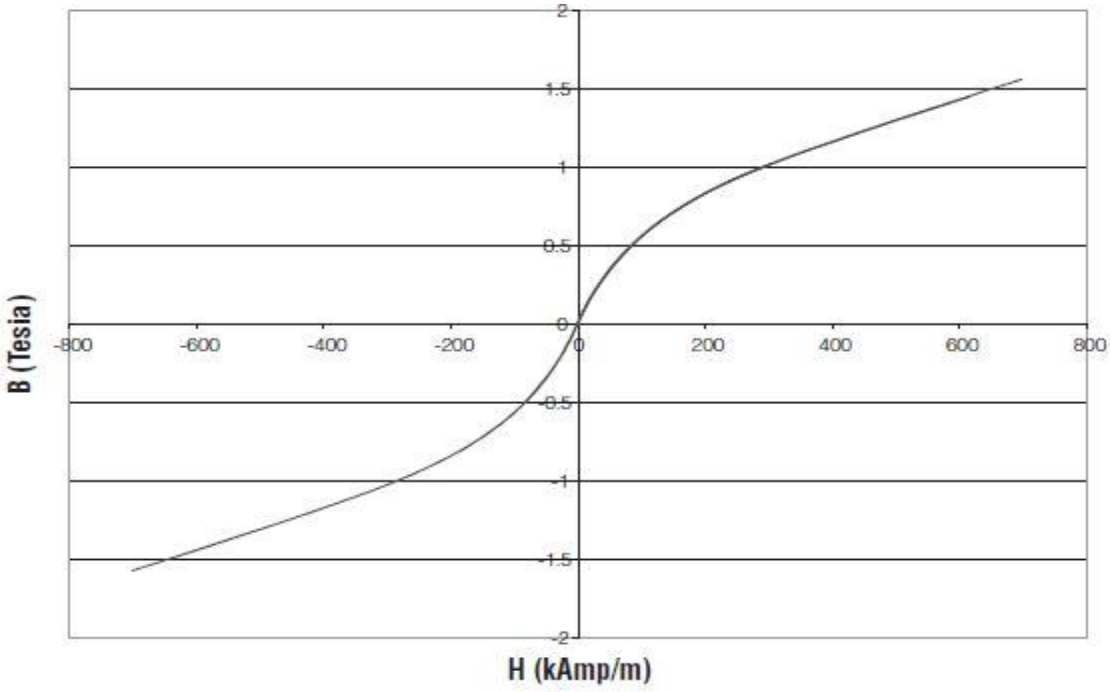

Fig.3.3 B H Curve MRF132DG

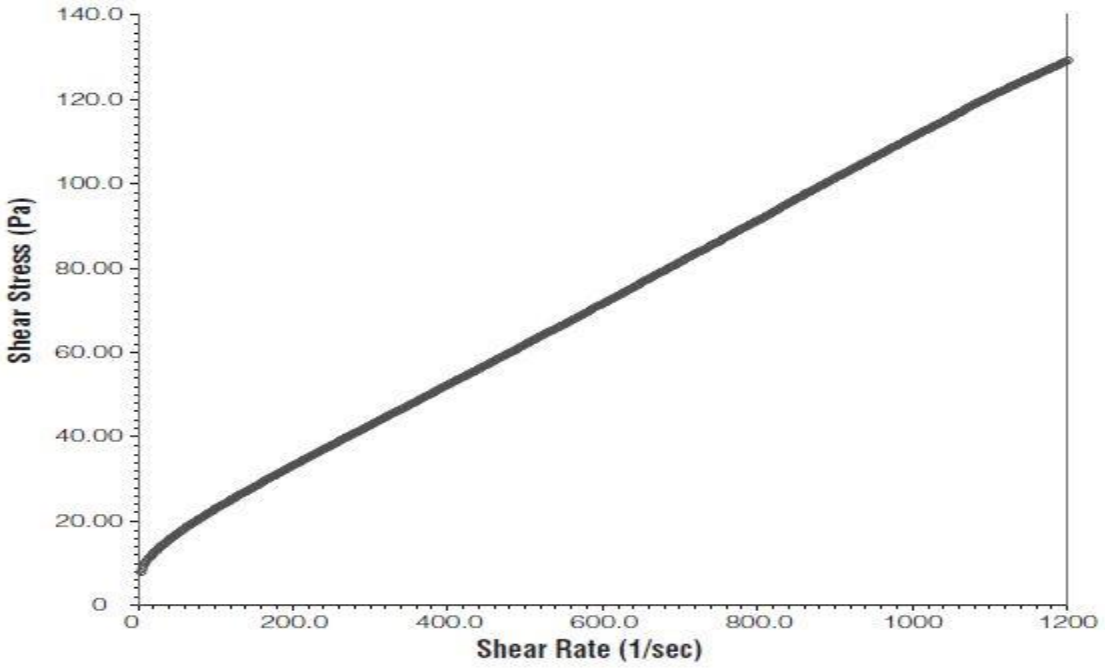

Fig.3.4 Shear stress VS Shear rate

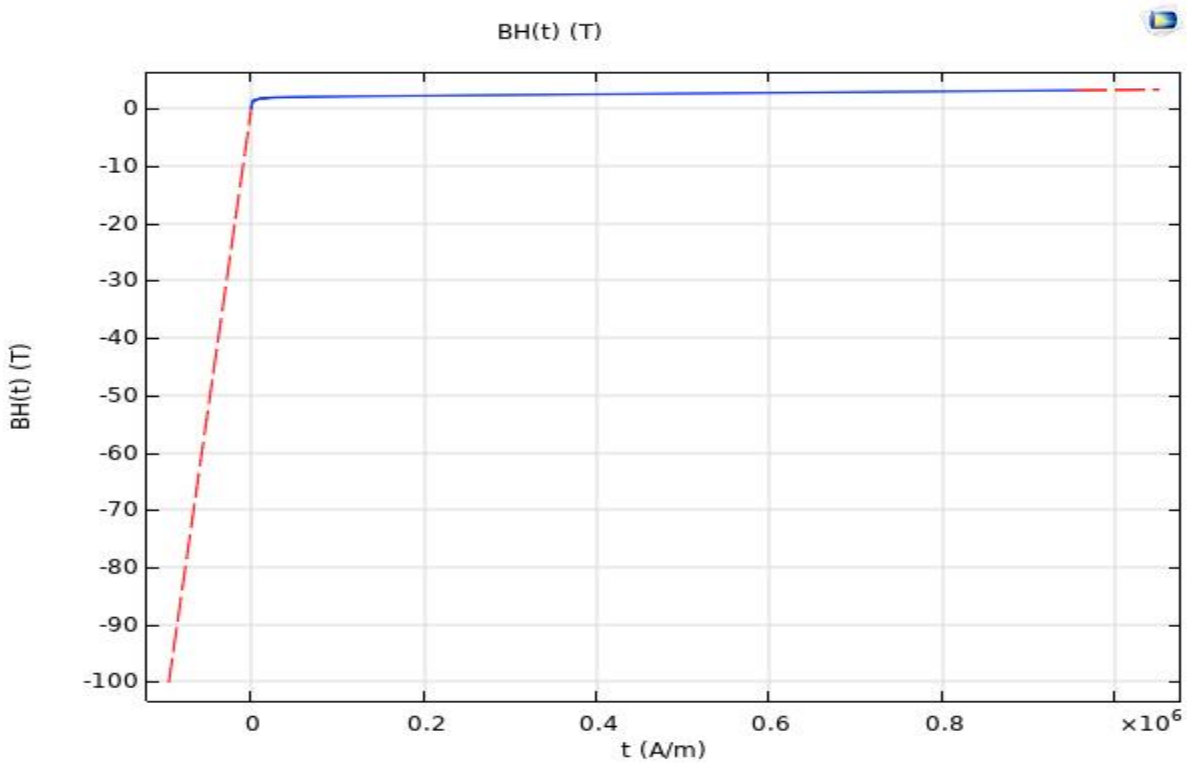

Fig.3.5 B H Curve AISI 1018 steel

Table 3.2 Properties of MRF 132DG

Property	**Values**
Physical Colour	Dark Gray Liquid
Viscosity, Pa-s @ 40°C (104°F)	0.112 ± 0.02
Density, g/cm^3	2.95-3.15
Operating Temperature, °C (°F)	-40 to +130 (-40 to +266)

3.3 SELECTION OF MULTIPHYSICS

To determine the magnetic field characteristic produced with the coil in COMSOL Multiphysics AC/DC module is added and magnetic field module(mf) submodule is selected. The governing equations of electromagnetism, are Maxwell's equation and Ampere's law, are included in the COMSOL solver. The equations solved are as follows: -

$$\nabla \times H = J + \frac{\partial D}{\partial t} \quad (1)$$

$$\nabla \cdot B = 0 \quad (2)$$

Where B, J, H and D, are the magnetic flux density, current density, magnetic field and electric displacement field.

For giving fluid properties for MRF region CFD module is added and laminar submodule is added. The weakly compressible Navier-Stokes equation is used to describe the magnetorheological fluid flows in the MRD. The reason for selection of laminar is because of the weakly compressible flow [23]. The viscosity of the MR fluid and the magnetic induction intensity are used to characterize, the relationship between flow and electromagnetic fields in the MRD. Consequently, the approach taken in this study's solution is to first determine the distribution of magnetic induction intensity

then load the resulting magnetic induction intensity distribution in an electromagnetic field as the starting points for solving the flow field problem. The modified Bingham fluid is used for modelling the dynamic viscosity of the MR fluid.

$$\eta = \eta_0 + \frac{\tau_y(B)}{\dot{\gamma}}\left[1 - e^{(-m\dot{\gamma})}\right] \quad (3)$$

Where m is model parameter, $\dot{\gamma}$ shear rate, η_0 zero field viscosity, $\tau_y(B)$ yield stress occurring with the magnetic field.

Shear stress and magnetic induction intensity relationship of MRF132DG is given by: -

$$\tau_y(B)=52.962B^4-176.51B^3+158.79B^2+13.708B+.1442 \quad (4)$$

3.4 ADDING BOUNDARY CONDITIONS

Axisymmetric boundary condition was added in the Magnetic Fields (mf) module and in laminar flow(spf) module. B H curve of MRF 132DG is added to the magnetization model under Ampere's law for MR fluid region. Multiturn copper coil was used for representing solenoid under the coil node. Variable current (I) is also defined so as to give varying input current which will then generate current in coil. Simulation was run with a stationary study and auxiliary using varying current from 1.5A, 2A, 2.5A, 3A, 3.5A, 4A for magneto static calculation. Magnetic field perpendicular to the coil was generated. Air boundary was used for magnetic insulation for the model.

Under the laminar flow(spf) a non-slip flow for the wall is provided as the boundary condition for the flow area in contact with the piston and cylinder. Non-Newtonian fluid property is added and for the dynamic viscosity generation yield stress and magnetic induction intensity is defined.

3.5 MESHING

A physics-controlled mesh is added for the meshing the entire geometry. Finer mesh is added as an input for the physics-controlled meshing. For the fluid flow region i.e., for the interior wall region the mesh gets super fine. Number of elements is 19023 and number of vertices is 10425. The fig 3.7 shows more details on the mesh.

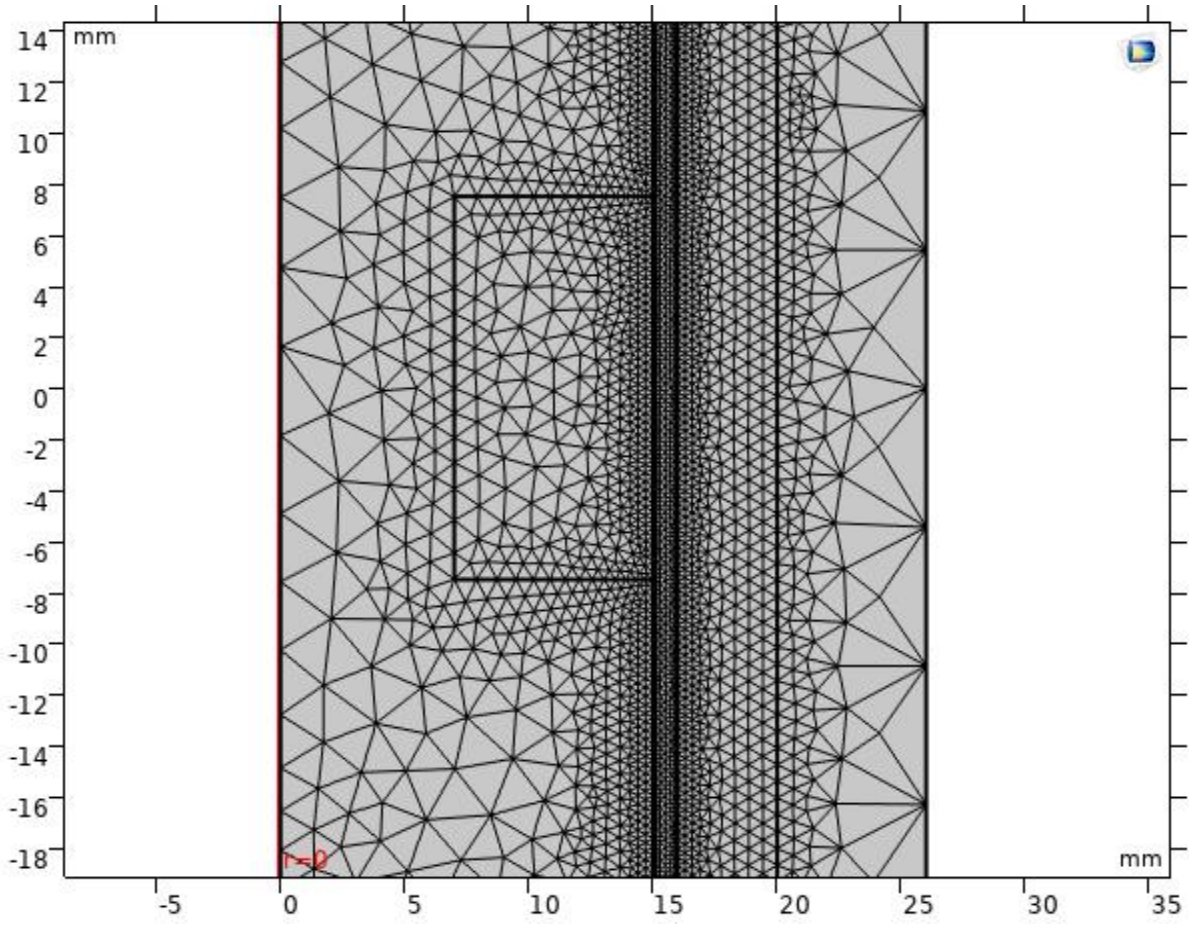

Fig.3.6 Meshed Output

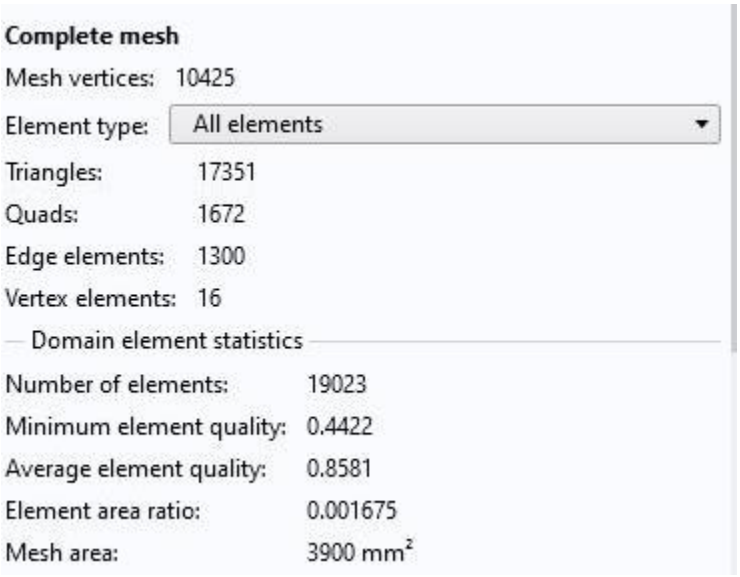

Fig.3.7 Mesh details for 1mm fluid flow gap

The change in the geometric parameters changes the mesh properties. For the fluid flow gap of 1.5mm there are 20192 elements and 11015 mesh vertices and the other properties are given in the figure 3.8. For the fluid flow gap of 2mm there are 21536 elements and 11689 mesh vertices and the other properties are given in the figure 3.9.

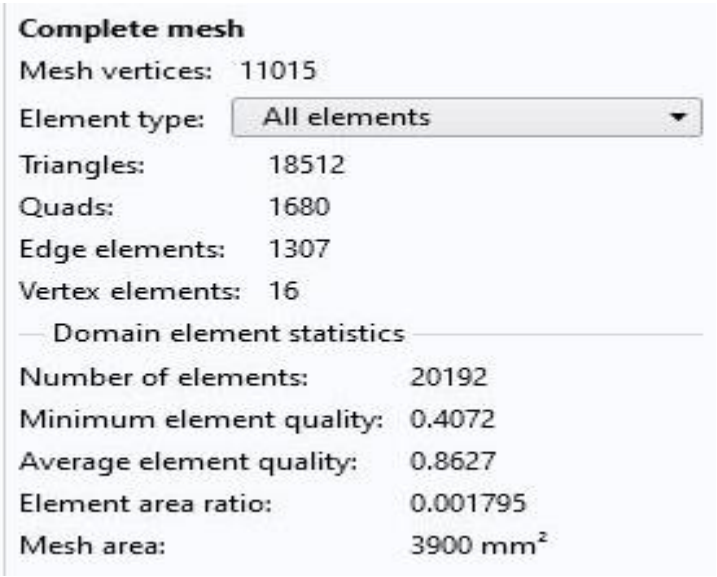

Fig.3.8 Mesh details for 1.5mm fluid flow gap

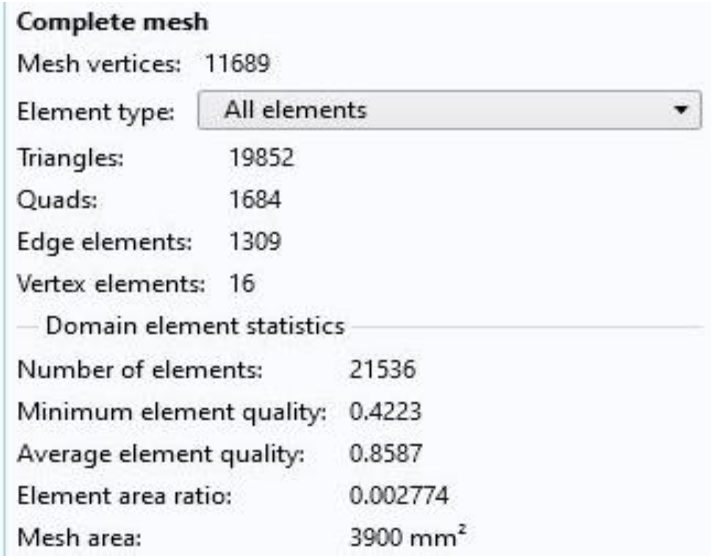

Fig.3.9 Mesh details for 2mm fluid flow gap

3.6 SOLVING

The problem is solved in the study node for the time independent stationary condition with magnetostatic condition. An auxiliary sweep is given in the study node for starts with 1.5A and a step of 0.5 and stop condition for 4 A. The solution generates for the current 1.5A, 2A, 2.5A, 3A, 3.5A, 4A. The magnetic field modules solve for Maxwells equation and laminar field module solves for Navier Stokes equation.

CHAPTER 4

RESULTS AND ANALYSIS

The solved results are postprocessed for the study requirement.MR fluid region is taken for magnetic flux density analysis, yield stress analysis and dynamic viscosity analysis for different coil turns number and varying gap size for MR fluid flow region.

4.1 MAGNETIC FLUX DENSITY ANALYSIS

Magnetic flux density for the number of turns in coil 300 for the currents 1.5A, 2A, 2.5A, 3A, 3.5A and 4A is given in the figure 4.1 and 4.2. Table 4.1 gives maximum magnetic flux density for the currents 1.5A, 2A, 2.5A, 3A, 3.5A and 4A for the coil turns number 300.

Table 4.1 Maximum magnetic flux density for different currents for 300 turns of coil

Current(A)	Magnetic flux density norm max (T)
1.5	1.862757
2	2.169693
2.5	2.450718
3	2.718114
3.5	2.973234
4	3.216696

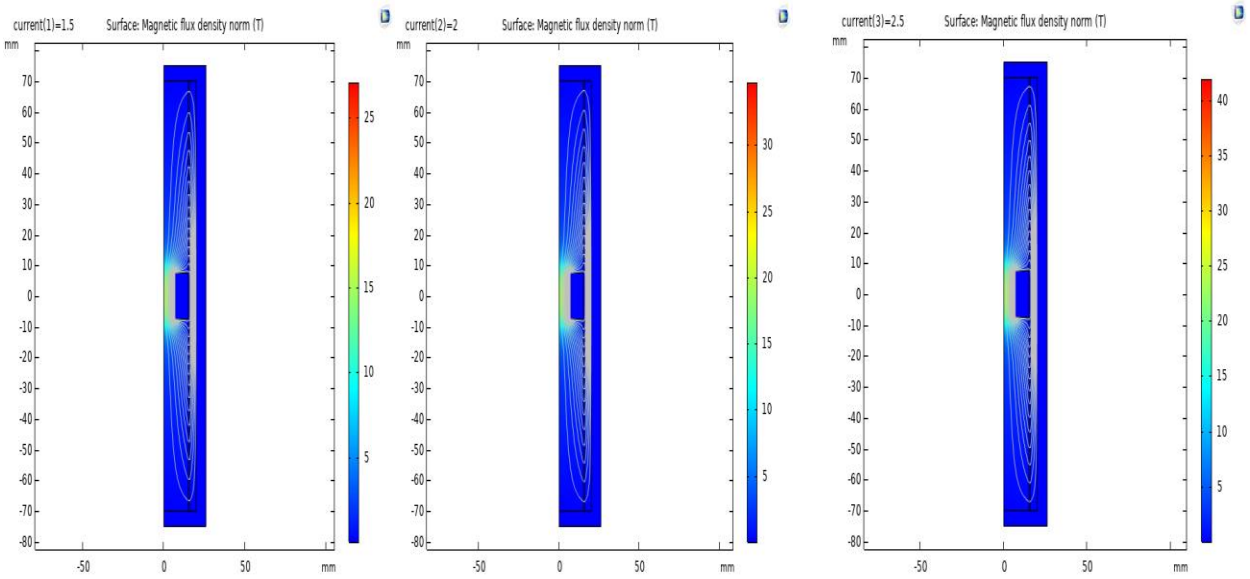

Fig.4.1 Magnetic flux density for the current 1.5A, 2A, 2.5A for 300 turns of coil

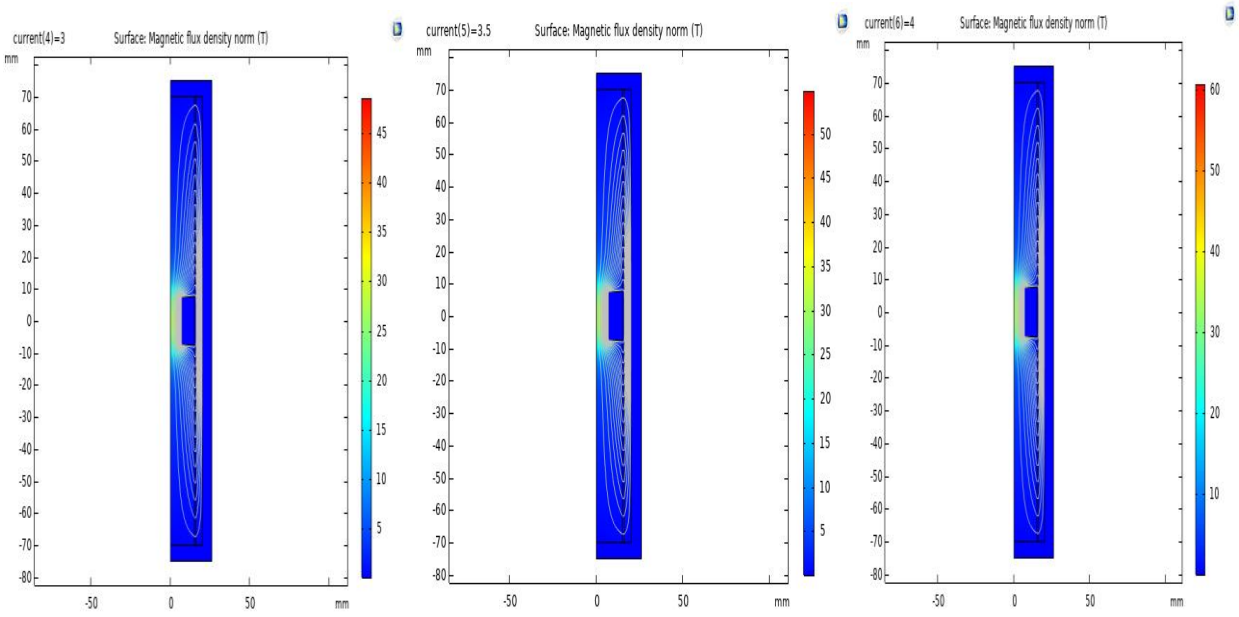

Fig.4.2 Magnetic flux density for the current 3A, 3.5A, 4A for 300 turns of coil

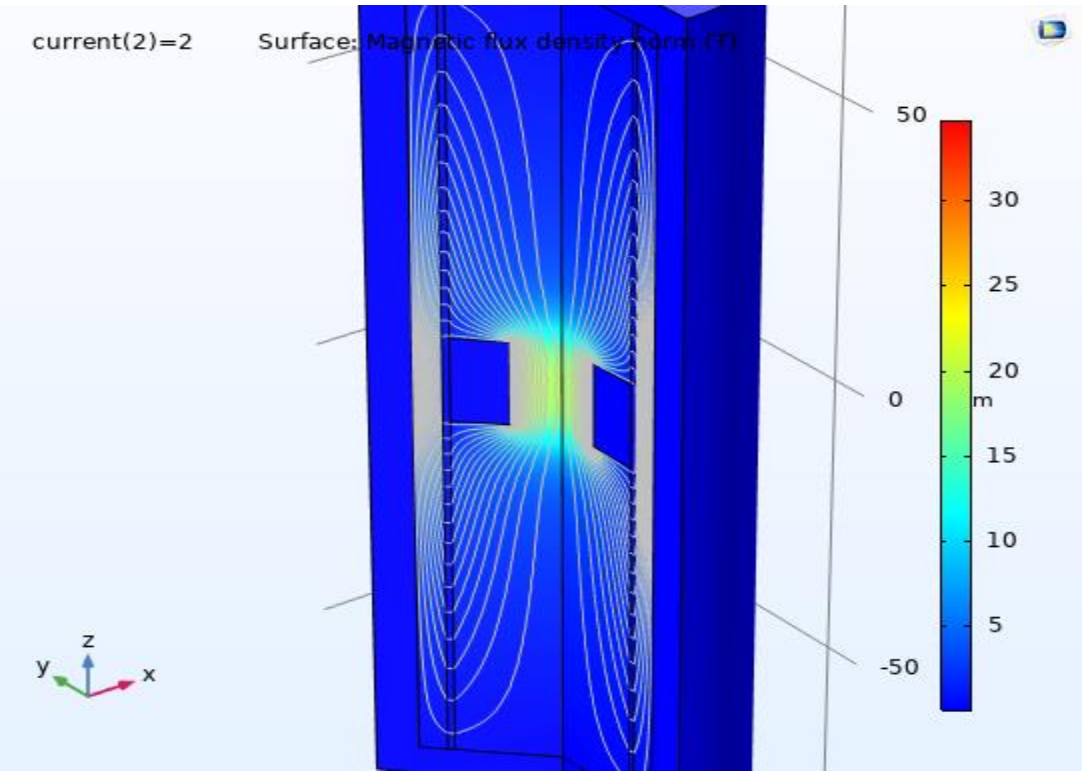

Fig.4.3 3-D view of magnetic flux density for current 2A for 300 turns of coil

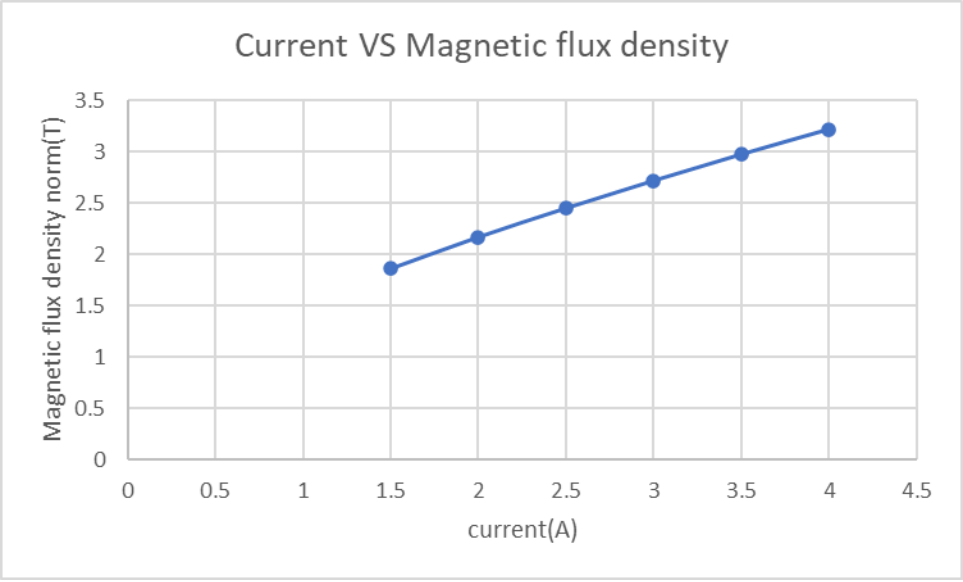

Fig 4.4 Current vs Magnetic flux density graph for 300 turns of coil

The magnetic flux density chart with respect to current shows that as the current increases the magnetic flux density at MR fluid also increases. The percentage of increase of magnetic flux density related to increase in current is shown in table 4.2.

Table 4.2 Percentage of increase of magnetic flux density related to increase in current

Current(A)	Percentage of increase of magnetic flux density
1.5A – 2A	16%
2A – 2.5A	13%
2.5A – 3A	11%
3A – 3.5A	9%
3.5A – 4A	8%
1.5A – 4A	73%

Percentage of increase of magnetic flux density is higher at lower current values for .5A increase is higher as compared to increased values of current. From 1.5A – 2A there is 16% increase in magnetic flux density and for 3.5A – 4A there is 8% increase in magnetic flux density. The Percentage of increase of magnetic flux density is 73% from 1.5A – 4A. The increase of percentage from 1.5A – 4A is high.

Magnetic flux density for the coil turns number 400 for the currents 1.5A, 2A, 2.5A, 3A, 3.5A and 4A is given in the figure 4.5 and 4.6. Table 4.3 gives maximum magnetic flux density for the currents 1.5A, 2A, 2.5A, 3A, 3.5A and 4A for the coil turns number 400.

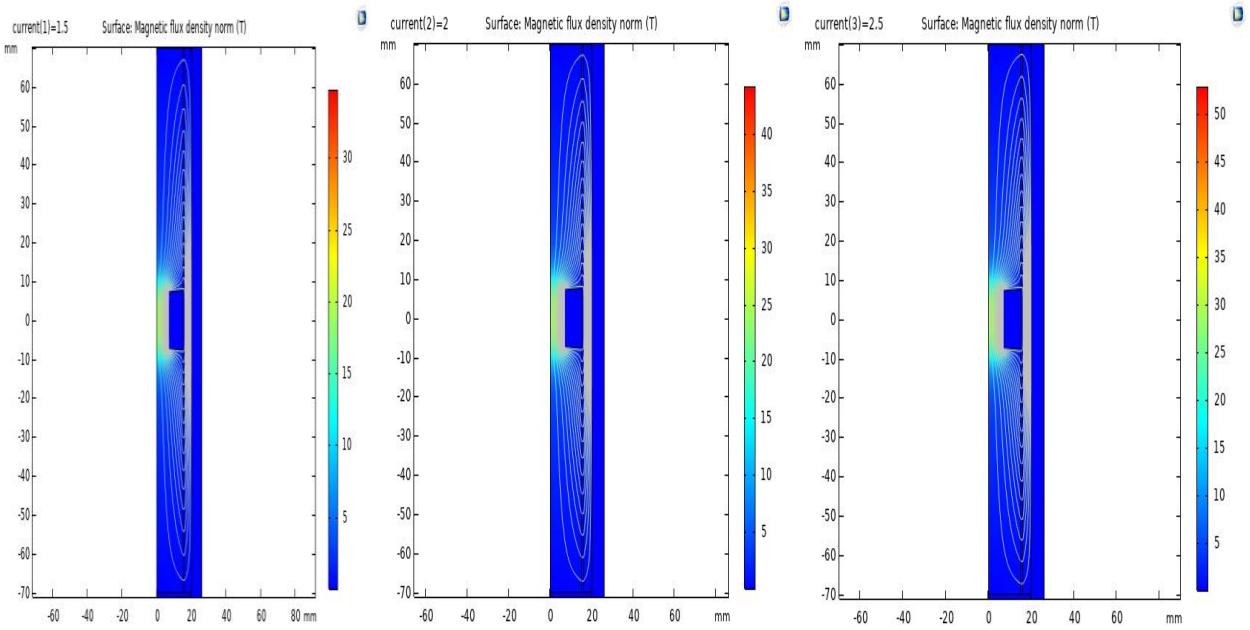

Fig.4.5 Magnetic flux density for the current 1.5A, 2A, 2.5A for 400 turns of coil

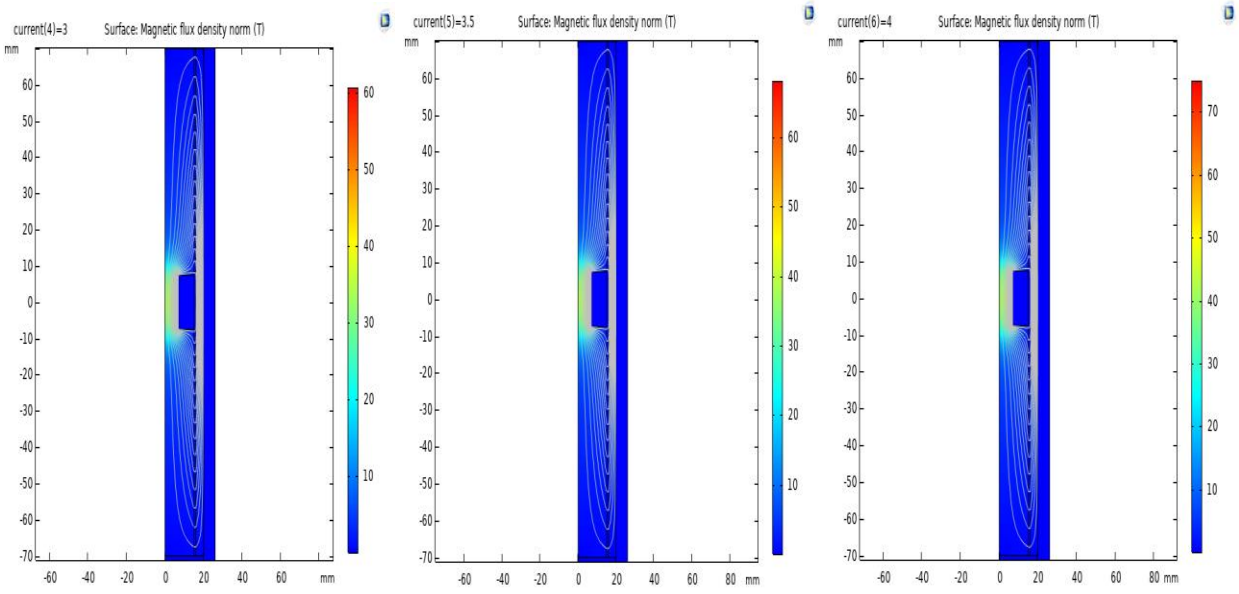

Fig.4.6 Magnetic flux density for the current 3A, 3.5A, 4A for 400 turns of coil

Table 4.3 Maximum magnetic flux density for different currents for 400 turns of coil

Current(A)	Magnetic flux density norm max (T)
1.5	2.169728
2	2.540407
2.5	2.889816
3	3.2167
3.5	3.531509
4	3.837047

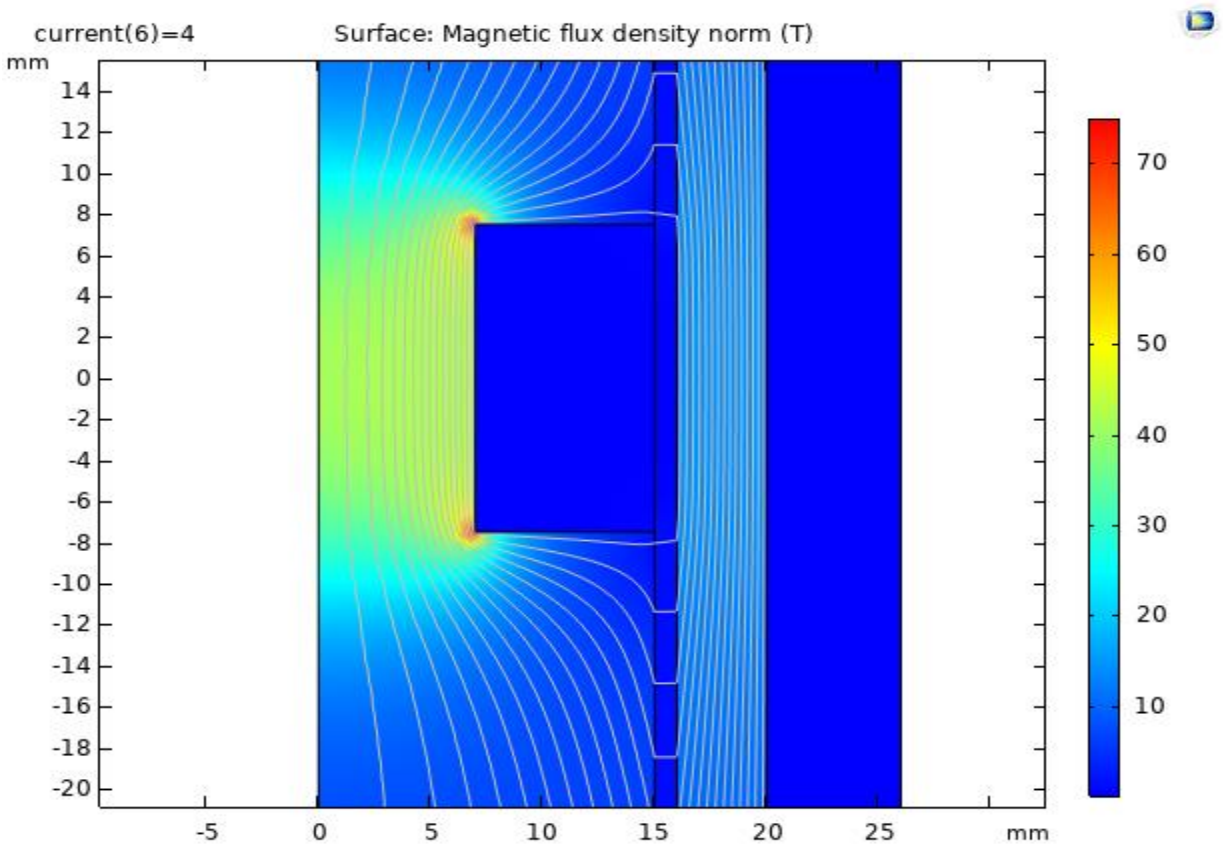

Fig.4.7 Magnetic flux density around coil for the current 4A for 400 turns of coil

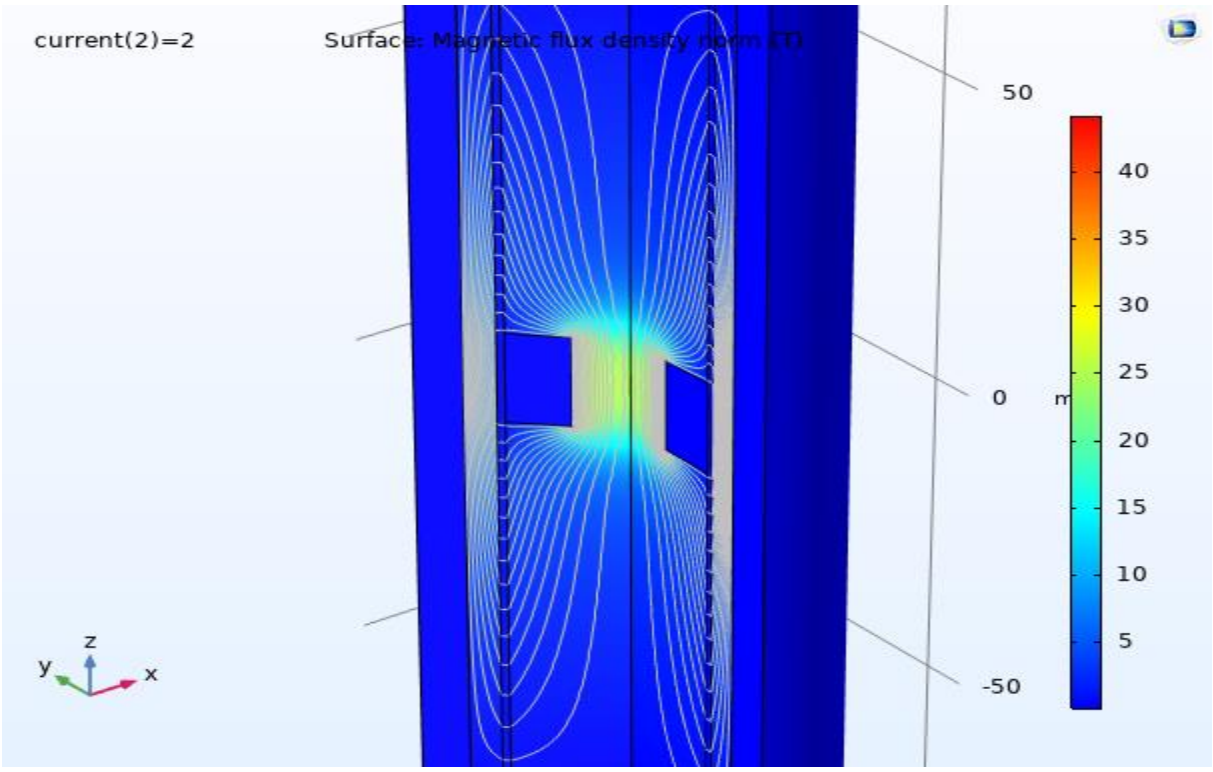

Fig.4.8 3-D view of magnetic flux density for current 2A for 400 turns of coil

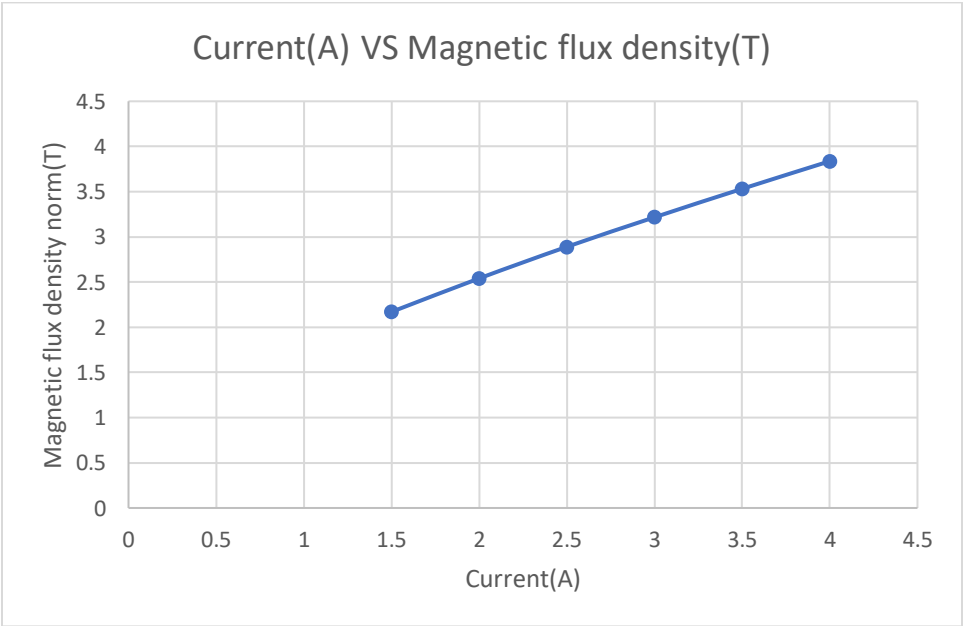

Fig.4.9 Current vs Magnetic flux density graph for 400 turns of coil

The magnetic flux density chart with respect to current shows that as the current increases the magnetic flux density at MR fluid also increases. The percentage of increase of magnetic flux density related to increase in current is shown in table 4.4.

Table 4.4 Percentage of increase of magnetic flux density related to increase in current

Current(A)	Percentage of increase of magnetic flux density
1.5A – 2A	17%
2A – 2.5A	14%
2.5A – 3A	11%
3A – 3.5A	10%
3.5A – 4A	9%
1.5A – 4A	77%

Percentage of increase of magnetic flux density is higher at lower current values for .5A increase is higher as compared to increased values of current. From 1.5A – 2A there is 17% increase in magnetic flux density and for 3.5A – 4A there is 9% increase in magnetic flux density. The Percentage of increase of magnetic flux density is 63% from 1.5A – 4A. The increase of percentage from 1.5A – 4A is high.

Magnetic flux density for the coil turns number 500 for the currents 1.5A, 2A, 2.5A, 3A, 3.5A and 4A is given in the figure 4.10 and 4.11. Table 4.5 gives maximum magnetic flux density for the currents 1.5A, 2A, 2.5A, 3A, 3.5A and 4A for the coil turns number 500.

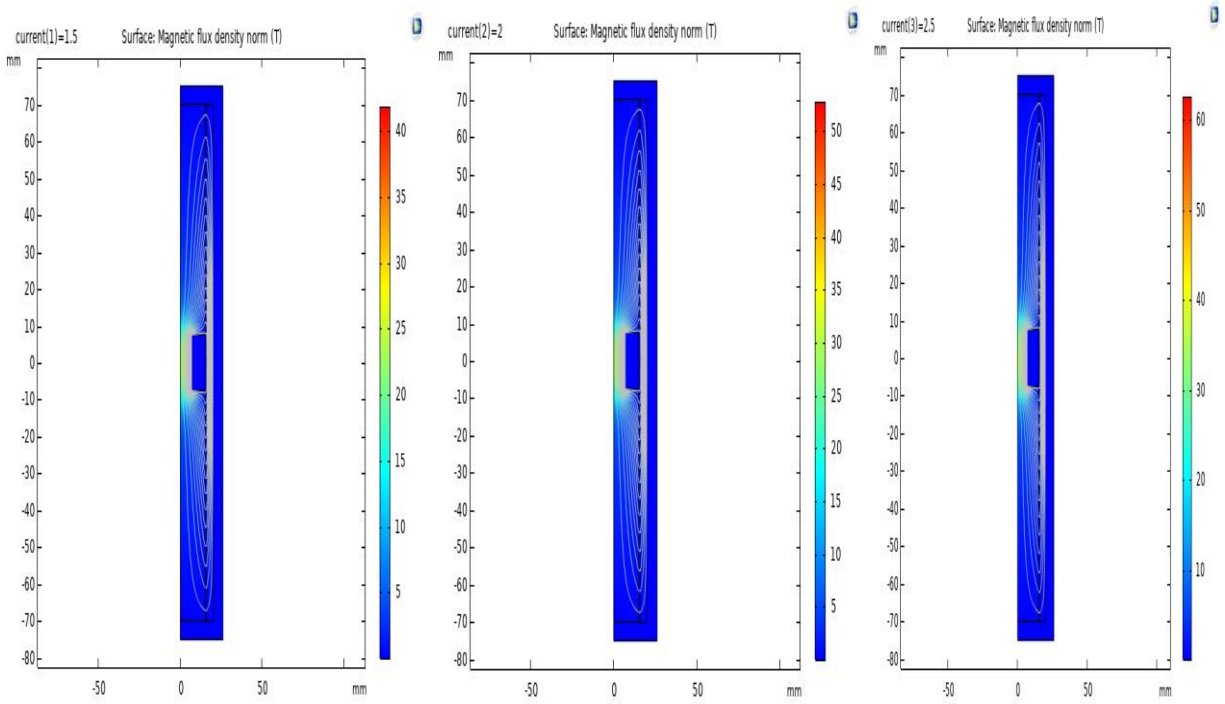

Fig.4.10 Magnetic flux density for the current 1.5A, 2A, 2.5A for 500 turns of coil

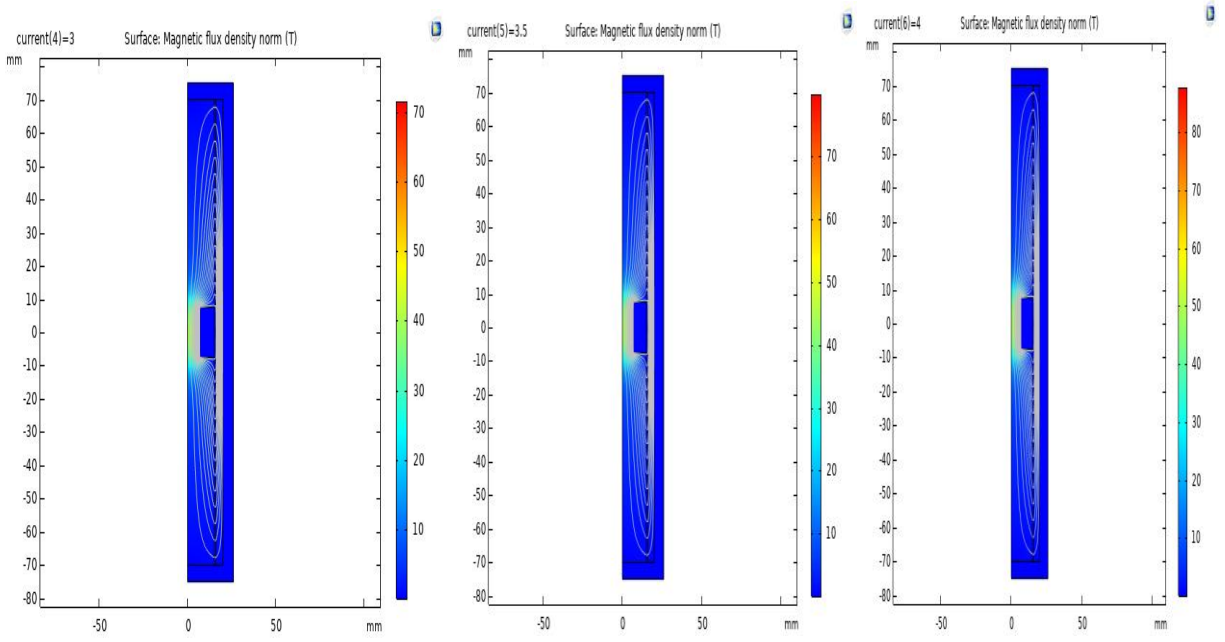

Fig.4.11 Magnetic flux density for the current 3A, 3.5A, 4A for 500 turns of coil

Table 4.5 Maximum magnetic flux density for different currents for 500 turns of coil

Current(A)	Magnetic flux density norm max (T)
1.5	2.450746
2	2.889799
2.5	3.296557
3	3.685305
3.5	4.061316
4	4.428324

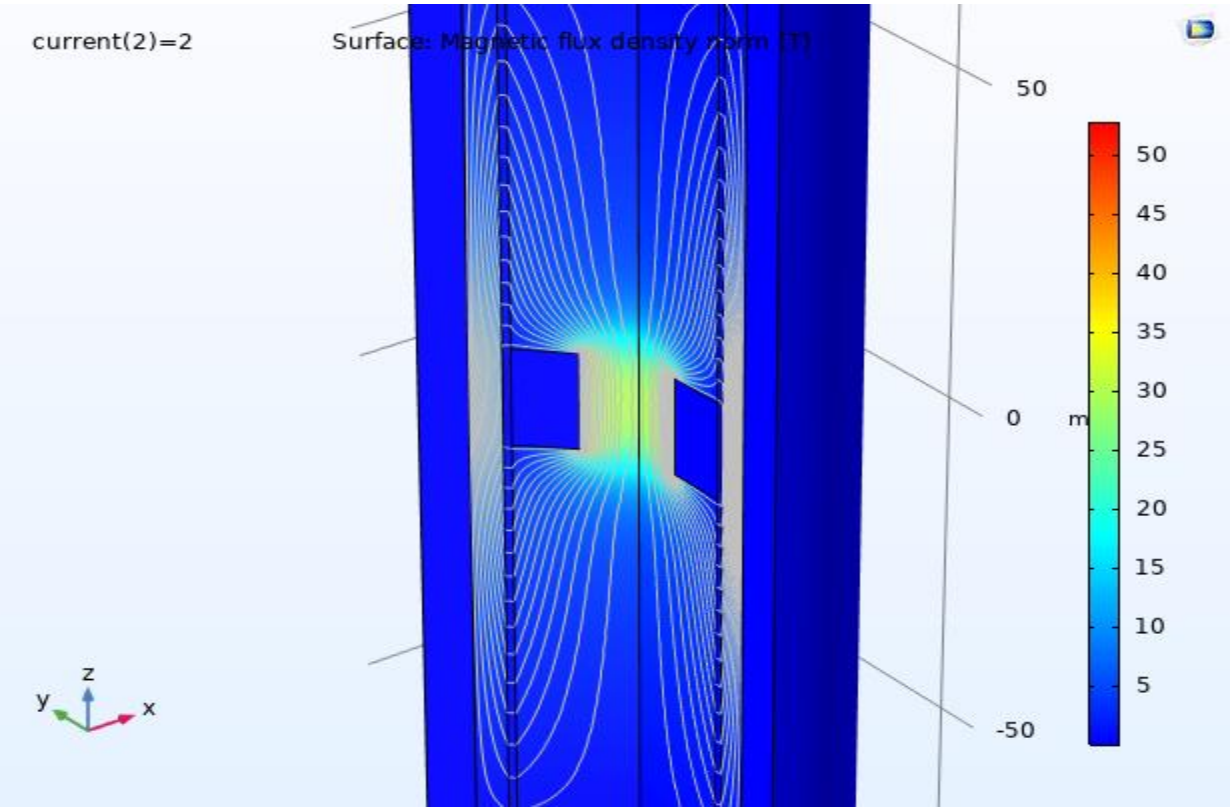

Fig.4.12 3-D view of magnetic flux density for current 2A for 500 turns of coil

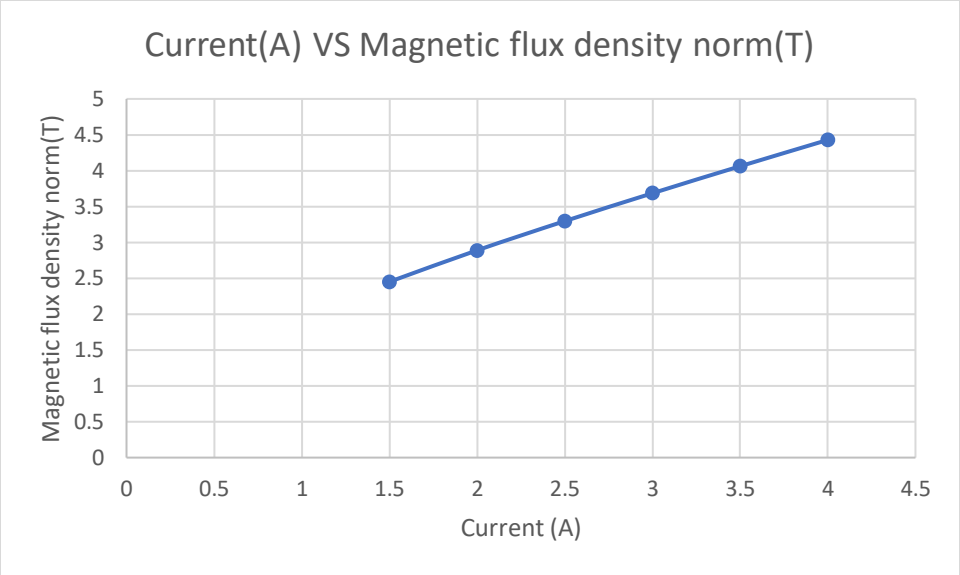

Fig.4.13 Current vs Magnetic flux density graph for 500 turns of coil

The magnetic flux density chart with respect to current shows that as the current increases the magnetic flux density at MR fluid also increases. The percentage of increase of magnetic flux density related to increase in current is shown in table 4.6.

Table 4.6 Percentage of increase of magnetic flux density related to increase in current

Current(A)	Percentage of increase of magnetic flux density
1.5A – 2A	18%
2A – 2.5A	14%
2.5A – 3A	12%
3A – 3.5A	10%
3.5A – 4A	9%
1.5A – 4A	81%

Percentage of increase of magnetic flux density is higher at lower current values for .5A increase is higher as compared to increased values of current. From 1.5A – 2A there is 18% increase in magnetic flux density and for 3.5A – 4A there is 9% increase in magnetic flux density. The Percentage of increase of magnetic flux density is 81% from 1.5A – 4A. The increase of percentage from 1.5A – 4A is high.

Magnetic flux density for the coil turns number 600 for the currents 1.5A, 2A, 2.5A, 3A, 3.5A and 4A is given in the figure 4.14 and 4.15. Table 4.7 gives maximum magnetic flux density for the currents 1.5A, 2A, 2.5A, 3A, 3.5A and 4A for the coil turns number 600.

Table 4.7 Maximum magnetic flux density for different currents for 600 turns of coil

Current(A)	Magnetic flux density norm max (T)
1.5	2.718176
2	3.216726
2.5	3.685307
3	4.135359
3.5	4.573015
4	5.000404

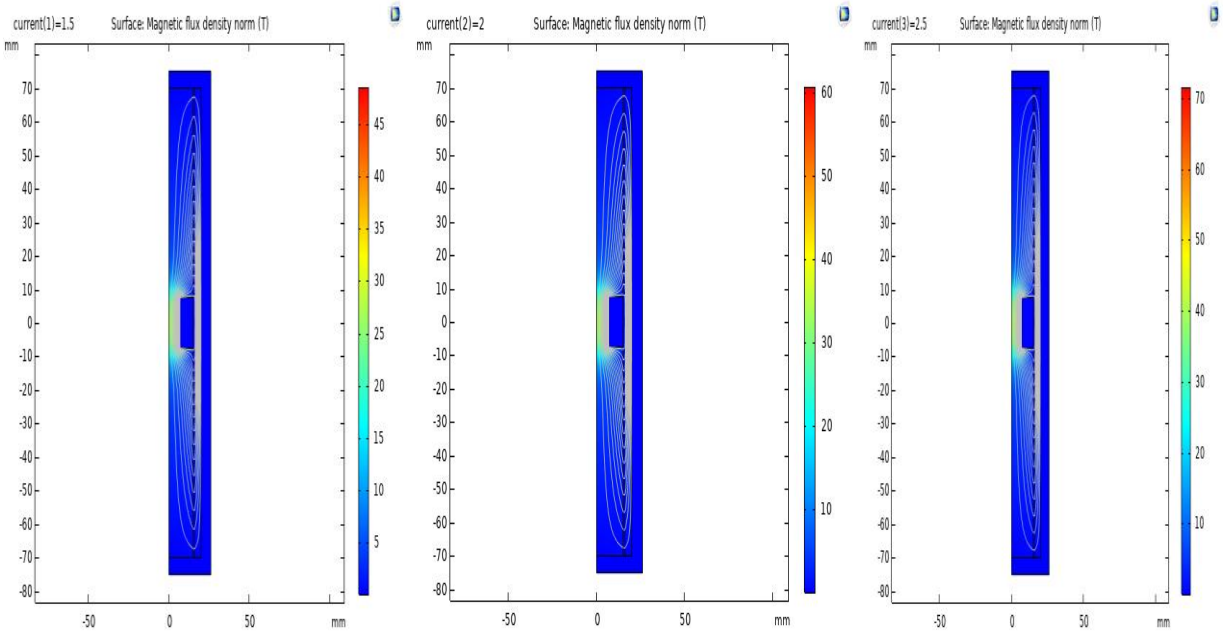

Fig.4.14 Magnetic flux density for the current 1.5A, 2A, 2.5A for 600 turns of coil

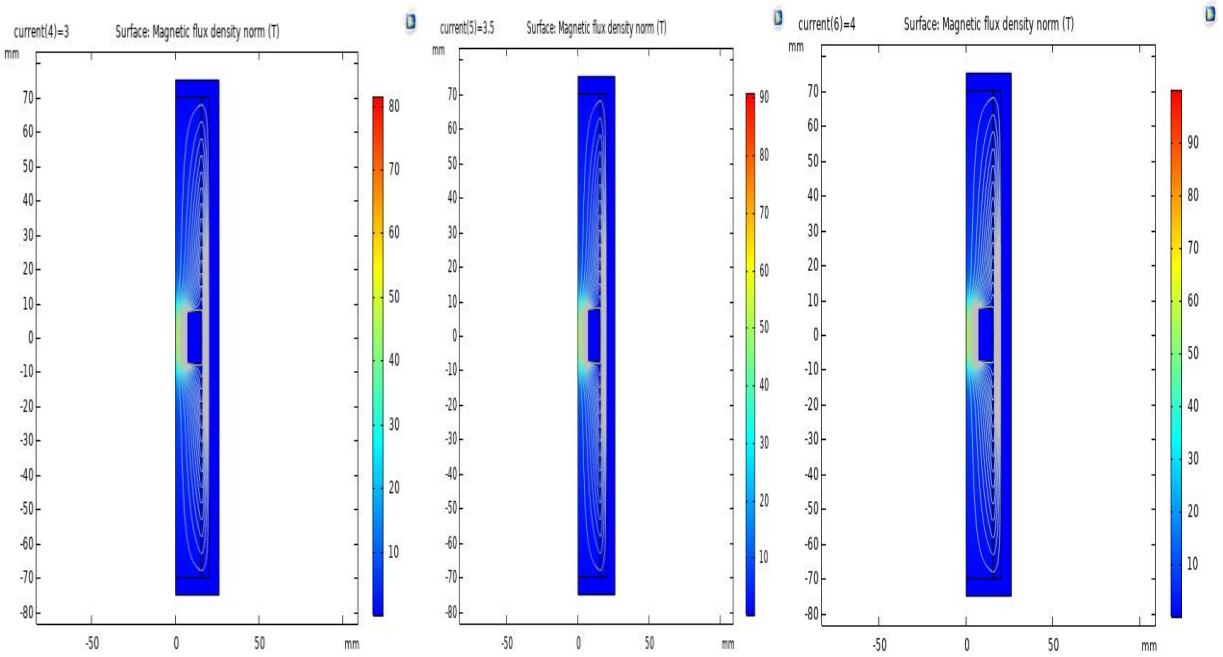

Fig.4.15 Magnetic flux density for the current 3A, 3.5A, 4A for 600 turns of coil

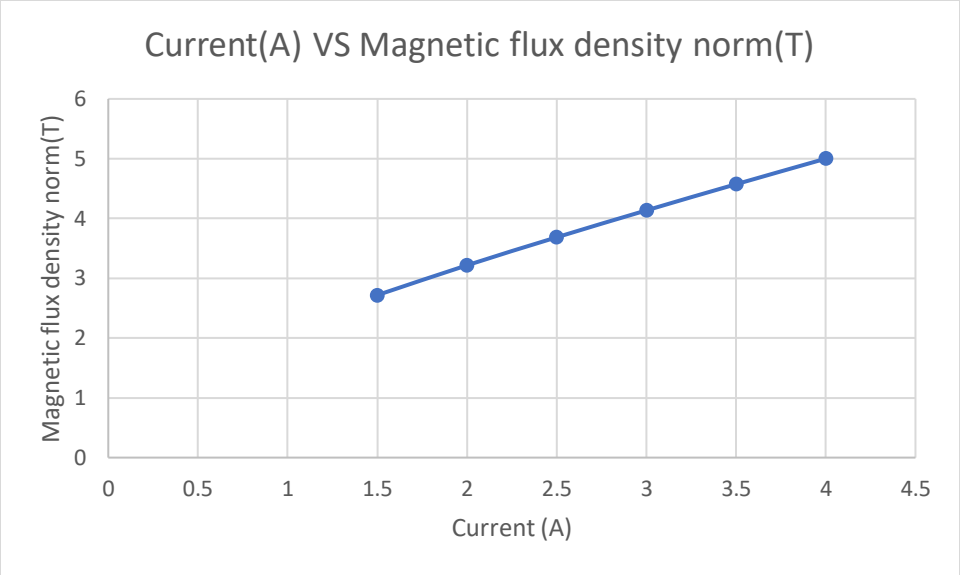

Fig.4.16 Current vs Magnetic flux density graph for 600 turns of coil

The magnetic flux density chart with respect to current shows that as the current increases the magnetic flux density at MR fluid also increases. The percentage of increase of magnetic flux density related to increase in current is shown in table 4.8.

Table 4.8 Percentage of increase of magnetic flux density related to increase in current

Current(A)	Percentage of increase of magnetic flux density
1.5A – 2A	18%
2A – 2.5A	15%
2.5A – 3A	12%
3A – 3.5A	11%
3.5A – 4A	9%
1.5A – 4A	84%

Percentage of increase of magnetic flux density is higher at lower current values for .5A increase is higher as compared to increased values of current. From 1.5A – 2A there is 18% increase in magnetic flux density and for 3.5A – 4A there is 9% increase in magnetic flux density. The Percentage of increase of magnetic flux density is 84% from 1.5A – 4A. The increase of percentage from 1.5A – 4A is high.

Comparison of magnetic flux density for the turns in coil number 300,400,500 and 600 with respect to the current is given in the figure 4.14.

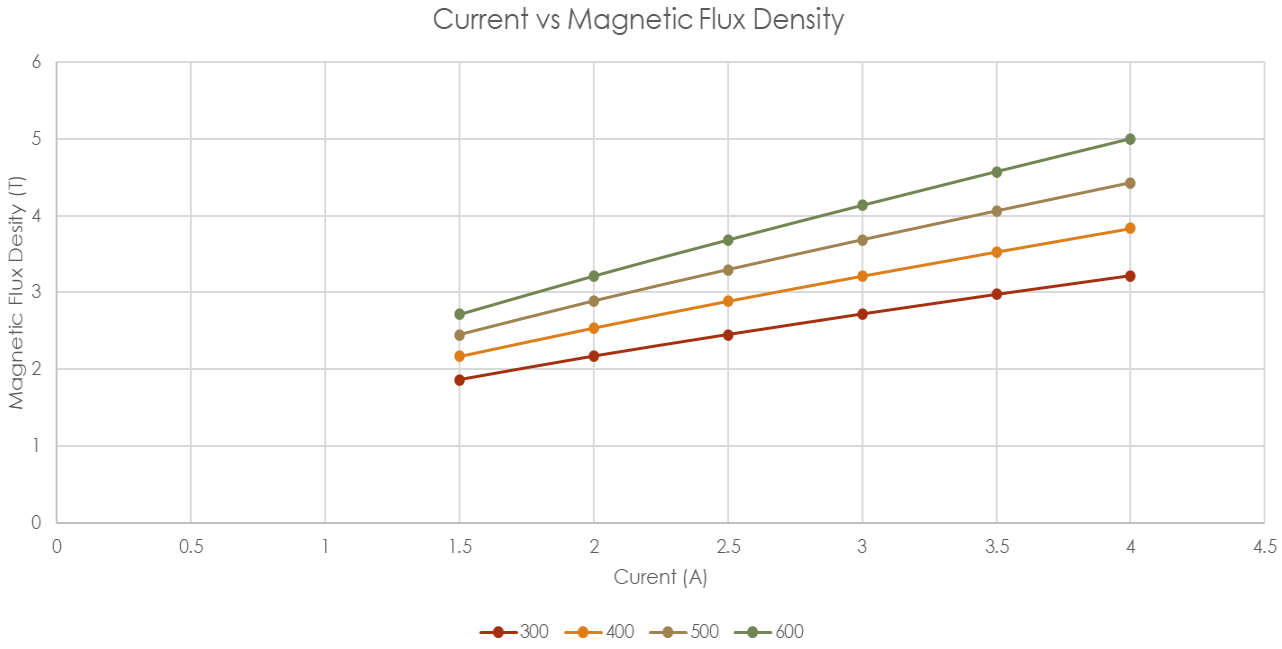

Fig.4.17 Current vs Magnetic flux density for number of turns coils

From the chart the inference is as the current is increased the magnetic flux density is also increasing in the MR fluid and when the coil turns number increases the magnetic flux density is also increasing proportionally. The Percentage of increase of magnetic flux density from 1.5A-4A for the coil turns number300,400,500 and 600 are73%,77%,81% and 84%. The increase in

percentage of increase of magnetic flux density for 1.5A from coil turns number 300 to 400 is 46% and for 4A from coil turns number 300 to 400 is 55%.

4.2 DYNAMIC VISCOSITY ANALYSIS

Dynamic viscosity for the currents 1.5A, 2A, 2.5A, 3A, 3.5A and 4A for the coil turns number 300, the chart is obtained after the simulation and is shown in the figure 4.15.

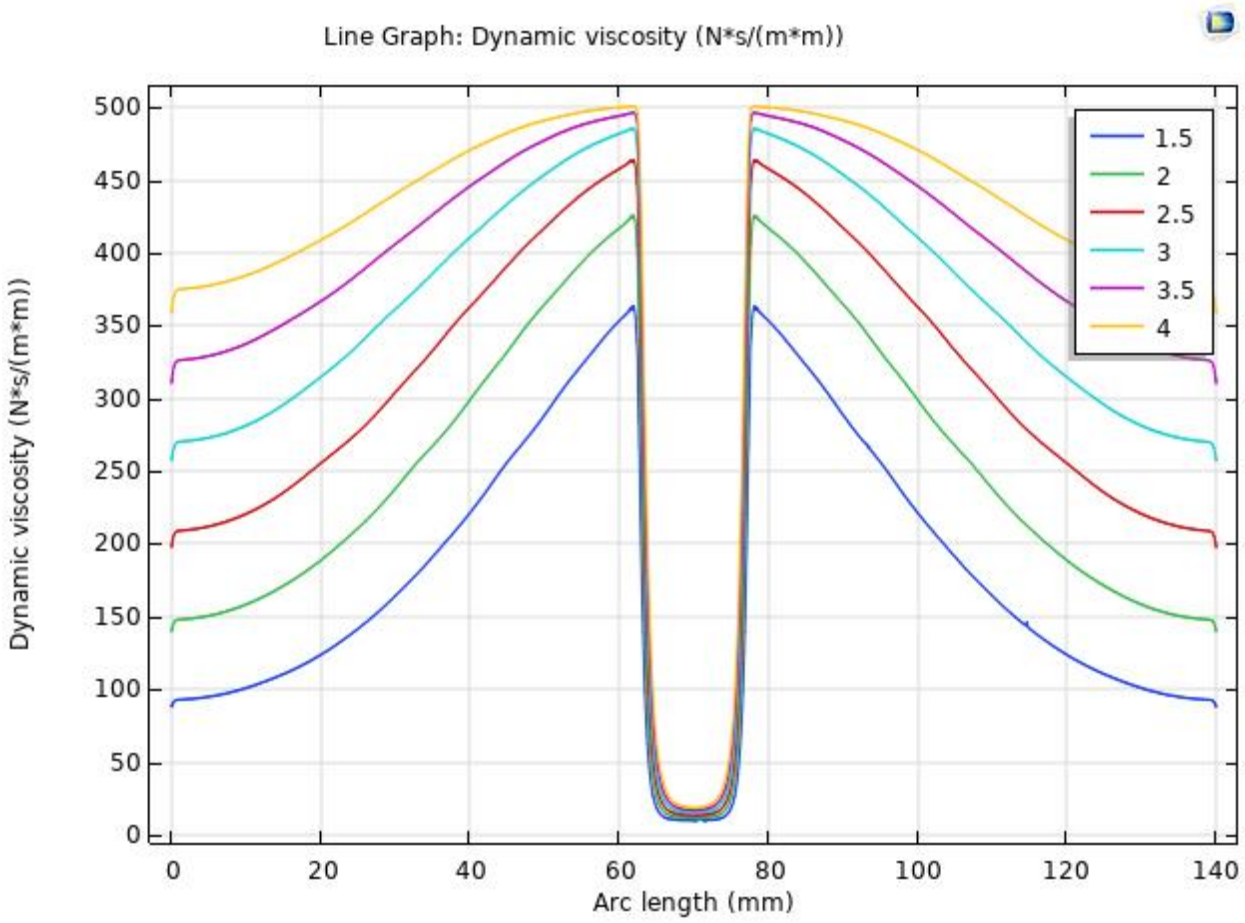

Fig.4.18 Dynamic viscosity for different currents for 300 turns of coil

The line graph shows that the maximum dynamic viscosity is at the effective magnetic poles of the damper. The dynamic viscosity over the length increases as the current increases.

The maximum dynamic viscosity for 1.5A current is 360 Ns/m^2, 2A current is 420 Ns/m^2,2.5A current is 460 Ns/m^2, 3A current is 480 Ns/m^2, 3.5A current is 490 Ns/m^2 and 4A current is 500 Ns/m^2.

Dynamic viscosity for the currents 1.5A, 2A, 2.5A, 3A, 3.5A and 4A for the coil turns number 400, the chart is obtained after the simulation and is shown in the figure 4.16.

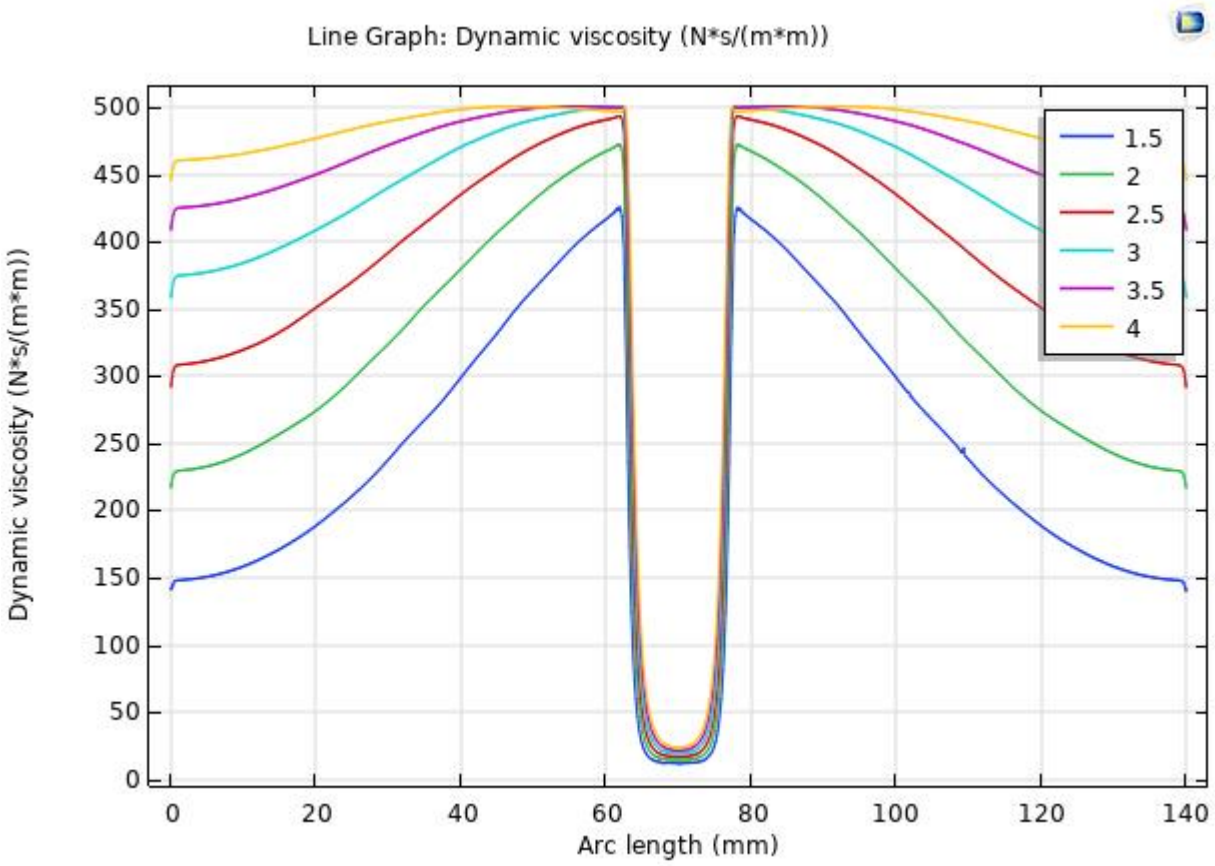

Fig.4.19 Dynamic viscosity for different currents for 400 turns of coil

The line graph shows that the maximum dynamic viscosity is at the effective magnetic poles of the damper. The dynamic viscosity over the length increases as the current increases.

The maximum dynamic viscosity for 1.5A current is 420 Ns/m^2, 2A current is 470 Ns/m^2,2.5A current is 495 Ns/m^2, 3A current is 498 Ns/m^2, 3.5A current is 499 Ns/m^2 and 4A current is 500 Ns/m^2.

Dynamic viscosity for the currents 1.5A, 2A, 2.5A, 3A, 3.5A and 4A for the coil turns number 500, the chart is obtained after the simulation and is shown in the figure 4.17.

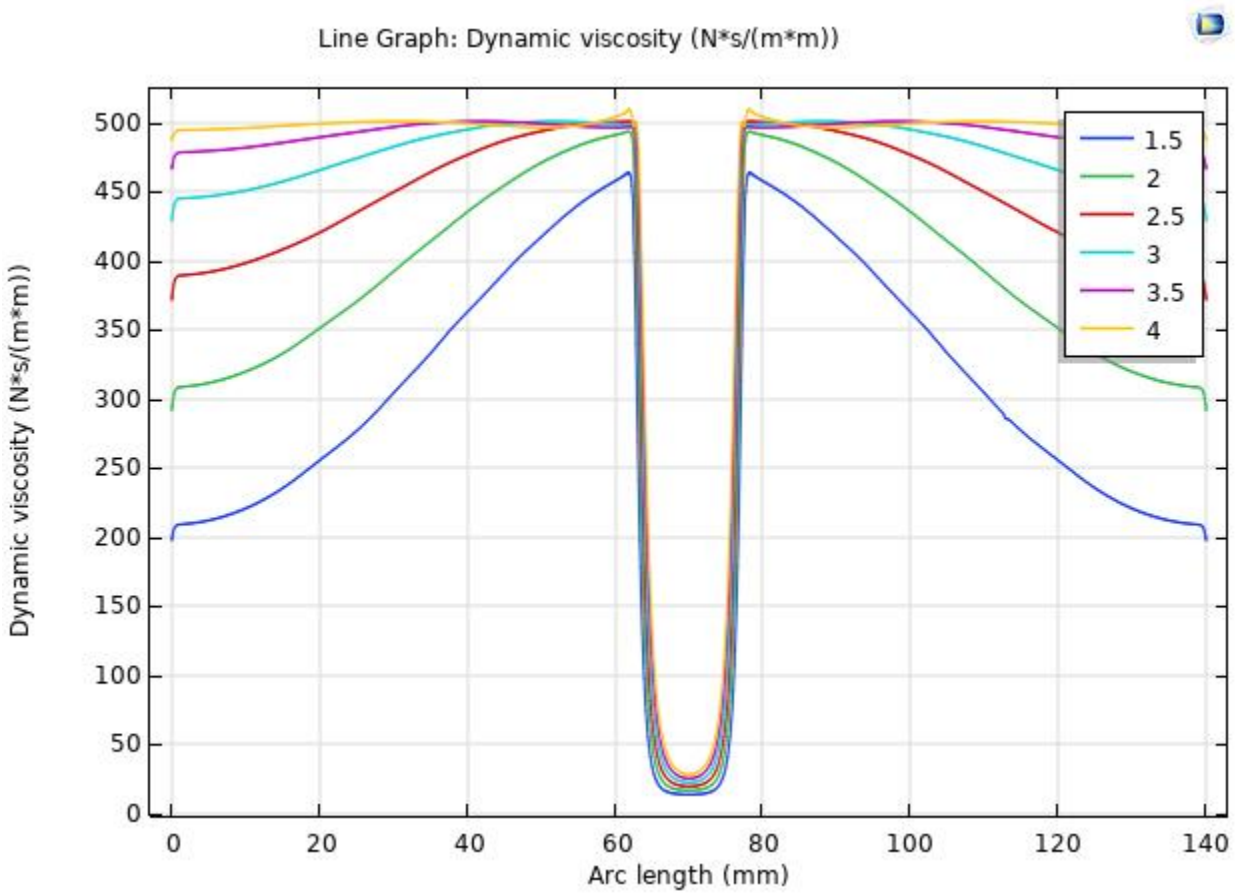

Fig.4.20 Dynamic viscosity for different currents for 500 turns of coil

The line graph shows that the maximum dynamic viscosity is at the effective magnetic poles of the damper. The dynamic viscosity over the length increases as the current increases.

The maximum dynamic viscosity for 1.5A current is 460 Ns/m^2, 2A current is 495 Ns/m^2,2.5A current is 497 Ns/m^2, 3A current is 498 Ns/m^2, 3.5A current is 500 Ns/m^2 and 4A current is 510 Ns/m^2.

Dynamic viscosity for the currents 1.5A, 2A, 2.5A, 3A, 3.5A and 4A for the coil turns number 600, the chart is obtained after the simulation and is shown in the figure 4.18.

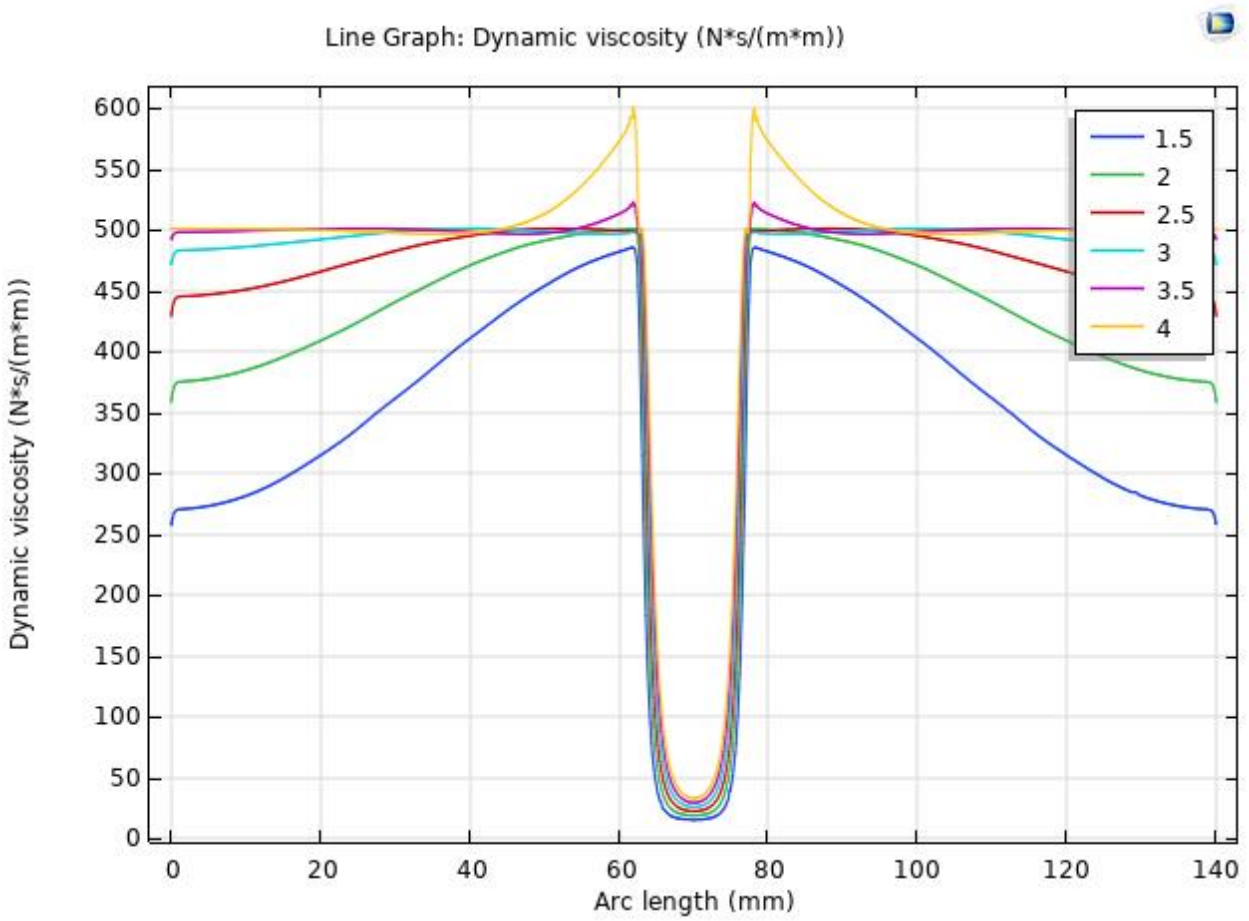

Fig.4.21 Dynamic viscosity for different currents for 600 turns of coil

The line graph shows that the maximum dynamic viscosity is at the effective magnetic poles of the damper. The dynamic viscosity over the length increases as the current increases.

The maximum dynamic viscosity for 1.5A current is 480 Ns/m^2, 2A current is 498 Ns/m^2,2.5A current is 499 Ns/m^2, 3A current is 500 Ns/m^2, 3.5A current is 520 Ns/m^2 and 4A current is 600 Ns/m^2. For the coil turns number 600 the dynamic viscosity is spiked up very high towards the magnetic poles compared to lower values of current.

Comparing the dynamic viscosities for different currents for different coil turns number as the coil turns number increases the dynamic viscosity also increases. The increase in percentage for the

dynamic viscosity from coil turns number300 to 600 for the current 1.5A is 33% and for the current 4A is 20%.

4.3 YIELD STRESS ANALYSIS

Yield stress analysis for viscosity for the currents 1.5A, 2A, 2.5A, 3A, 3.5A and 4A for the coil turns number 400, the chart is obtained after the simulation and is shown in the figure 4.18.

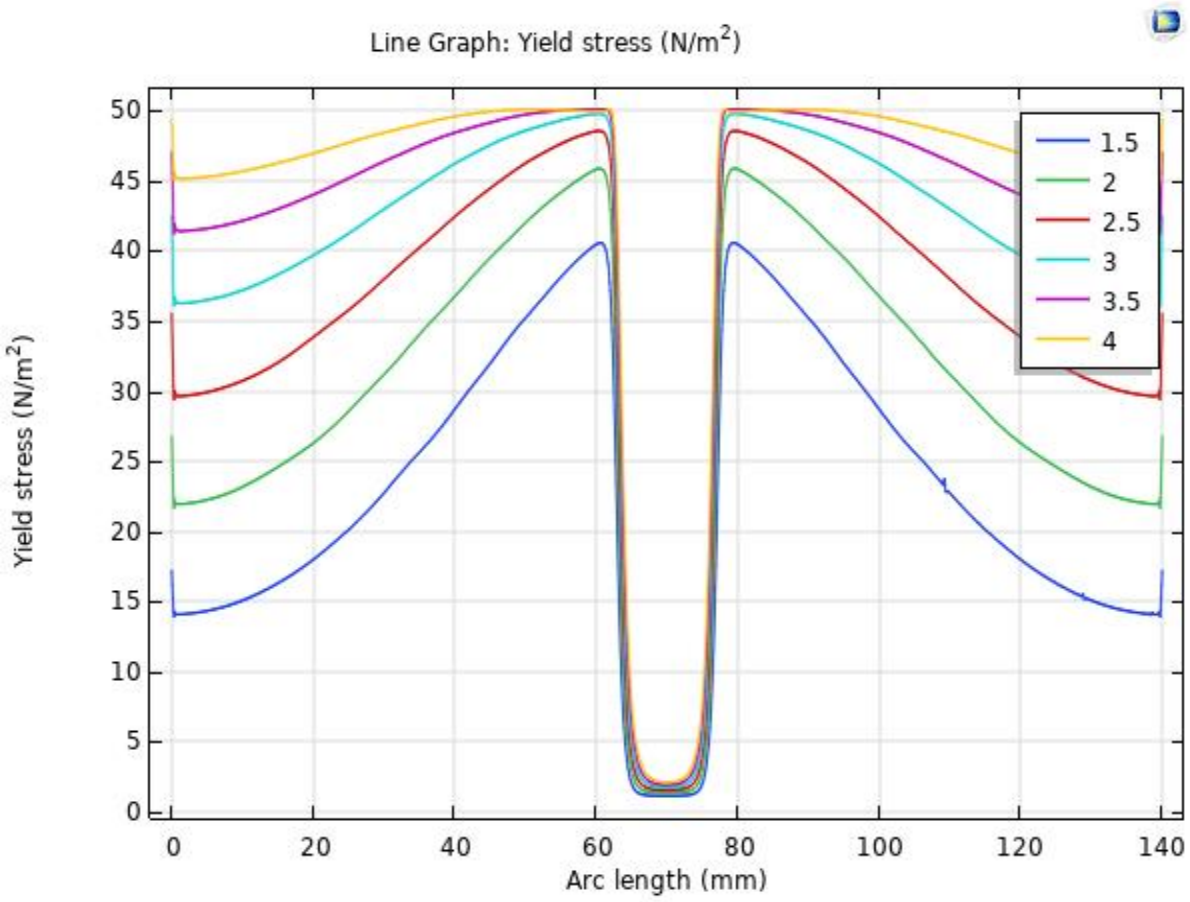

Fig.4.22 Yield stress for different currents for 400 turns of coil

The line graph shows that the maximum yield stress is at the effective magnetic poles of the damper. The yield stress over the length increases as the current increases.

The maximum yield stress for 1.5A current is 40 N/m^2, 2A current is 46 N/m^2,2.5A current is 48 N/m^2, 3A current is 49 N/m^2, 3.5A current is 50 N/m^2 and 4A current is 50 N/m^2.

Yield stress analysis for viscosity for the currents 1.5A, 2A, 2.5A, 3A, 3.5A and 4A for the coil turns number 500, the chart is obtained after the simulation and is shown in the figure 4.19.

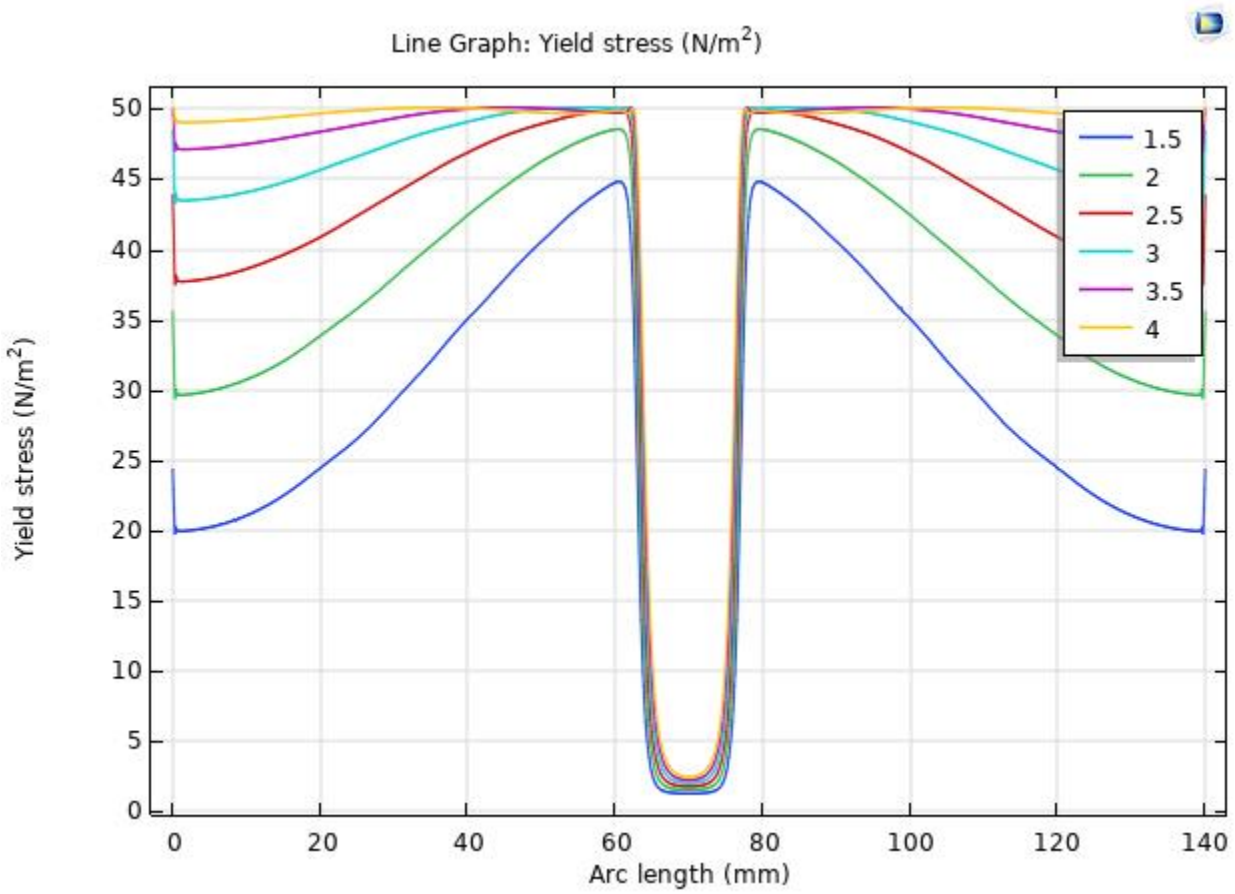

Fig.4.23 Yield stress for different currents for 500 turns of coil

The line graph shows that the maximum yield stress is at the effective magnetic poles of the damper. The yield stress over the length increases as the current increases.

The maximum yield stress for 1.5A current is 45 N/m^2, 2A current is 48 N/m^2,2.5A current is 49 N/m^2, 3A current is 49 N/m^2, 3.5A current is 50 N/m^2 and 4A current is 50 N/m^2.

Comparing the yield stresses for different currents for different coil turns number as the coil turns number increases the yield stress also increases.

4.4 INFLUENCE OF GAP WIDTH FOR MAGNETIC FLUX DENSITY

The gap width is varied from 1mm to 1.5mm and 2mm to find the influence on various parameter. The magnetic flux density for the gap 1mm,1,5mm and 2mm for the number of coil 400 and the currents 1.5A, 2A, 2.5A, 3A, 3.5A and 4A is shown in the table 4.9 and the chart for same is shown in the figure 4.19.

Table 4.9 Maximum magnetic flux density for different currents with varying the gap size

Current(A)	Magnetic flux density norm max (T) for the gap		
	1mm	1.5mm	2mm
1.5	2.169728	2.066683	1.987838
2	2.540407	2.414096	2.317023
2.5	2.889816	2.740575	2.626629
3	3.2167	3.046235	2.917572
3.5	3.531509	3.338752	3.194305
4	3.837047	3.618695	3.460085

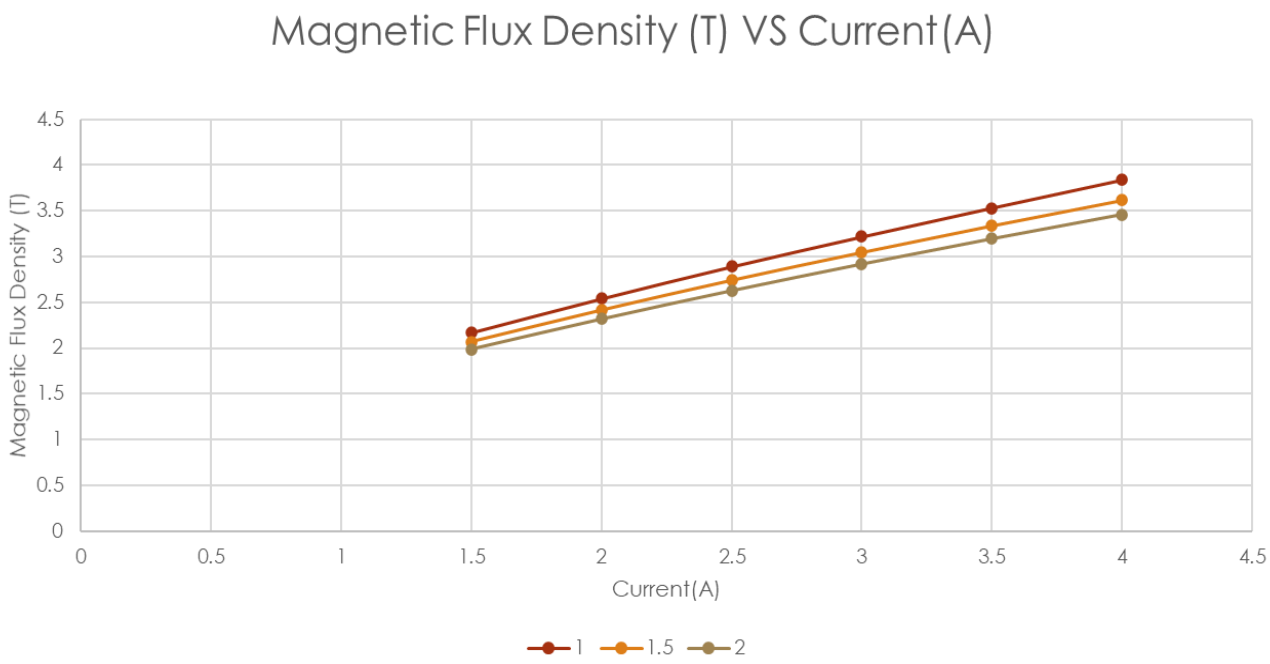

Fig.4.24 Current vs Magnetic flux density for coil turns number with varying gap size

The magnetic flux density is increased as the current increases even the gap is increased and the magnetic flux density decreases as the gap is increased for the same current. There is a decrease of 5% in magnetic flux density for 1.5A current for the change in gap from 1mm to 1.5mm, A decrease of 4% in magnetic flux density for 1.5A current for the change in gap from 1.5mm to 2mm and a decrease of 8% in magnetic flux density for 1.5A current for the change in gap from 1mm to 2mm.

There is a decrease of 6% in magnetic flux density for 4A current for the change in gap from 1mm to 1.5mm, A decrease of 4% in magnetic flux density for 4A current for the change in gap from 1.5mm to 2mm and a decrease of 10% in magnetic flux density for 4A current for the change in gap from 1mm to 2mm.The magnetic flux density decreases corresponding to the increase in gap size.

4.5 INFLUENCE OF GAP WIDTH FOR DYNAMIC VISCOSITY

The dynamic viscosity generated for the gap size 1.5mm and 2mm with coil turns number 400 for the currents 1.5A, 2A, 2.5A, 3A, 3.5A and 4A is shown in the figure 4.20 and figure 4.21.

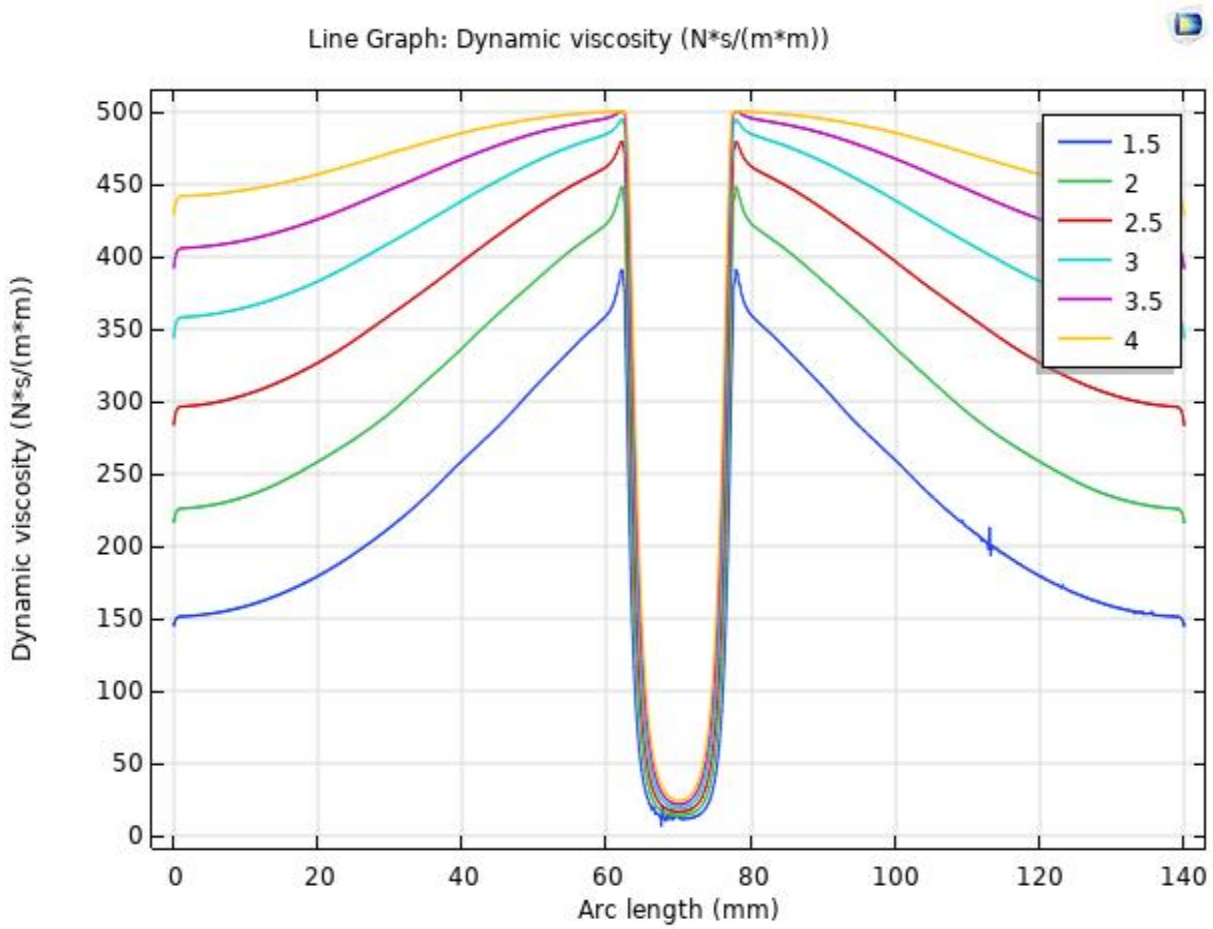

Fig.4.25 Dynamic viscosity for different currents with a gap size of 1.5mm

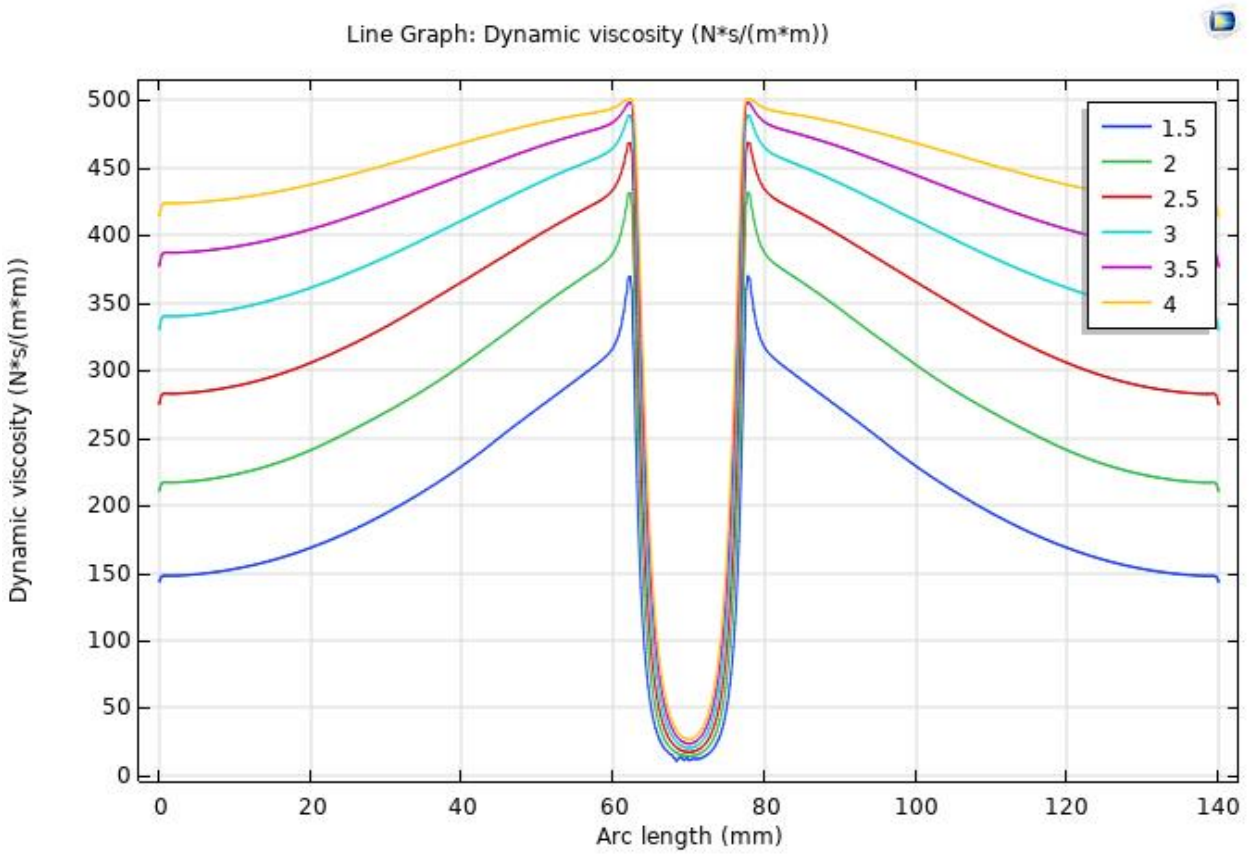

Fig.4.26 Dynamic viscosity for different currents with a gap size of 2mm

Comparing the dynamic viscosities for the gap sizes 1mm, 1.5mm and 2mm with coil turns number400 for the currents 1.5A, 2A, 2.5A, 3A, 3.5A and 4A the dynamic viscosity decreases with the increase in gap size of MR fluid flow region. Considering the current 1.5A for the gap size 1mm the maximum dynamic viscosity is 420 Ns/m^2, for 1.5mm gap size the maximum dynamic viscosity is 380 Ns/m^2 and for 2mm gap size the maximum dynamic viscosity is 360 Ns/m^2. The percentage of decrease of dynamic viscosity from 1mm gap to 2mm is 14%.

The viscosity decreases as the damping gap increases due to the decrease in the magnetic flux density. The damping effect decreases for the decrease in viscosity and as there by there is a need

for an optimum gap for an effective damping considering the damping force needed to accommodate by the MR damper.

4.6 INFLUENCE OF GAP WIDTH FOR YIELD STRESS

The yield stress generated for the gap size 1.5mm and 2mm with coil turns number 400 for the currents 1.5A, 2A, 2.5A, 3A, 3.5A and 4A is shown in the figure 4.22 and figure 4.23.

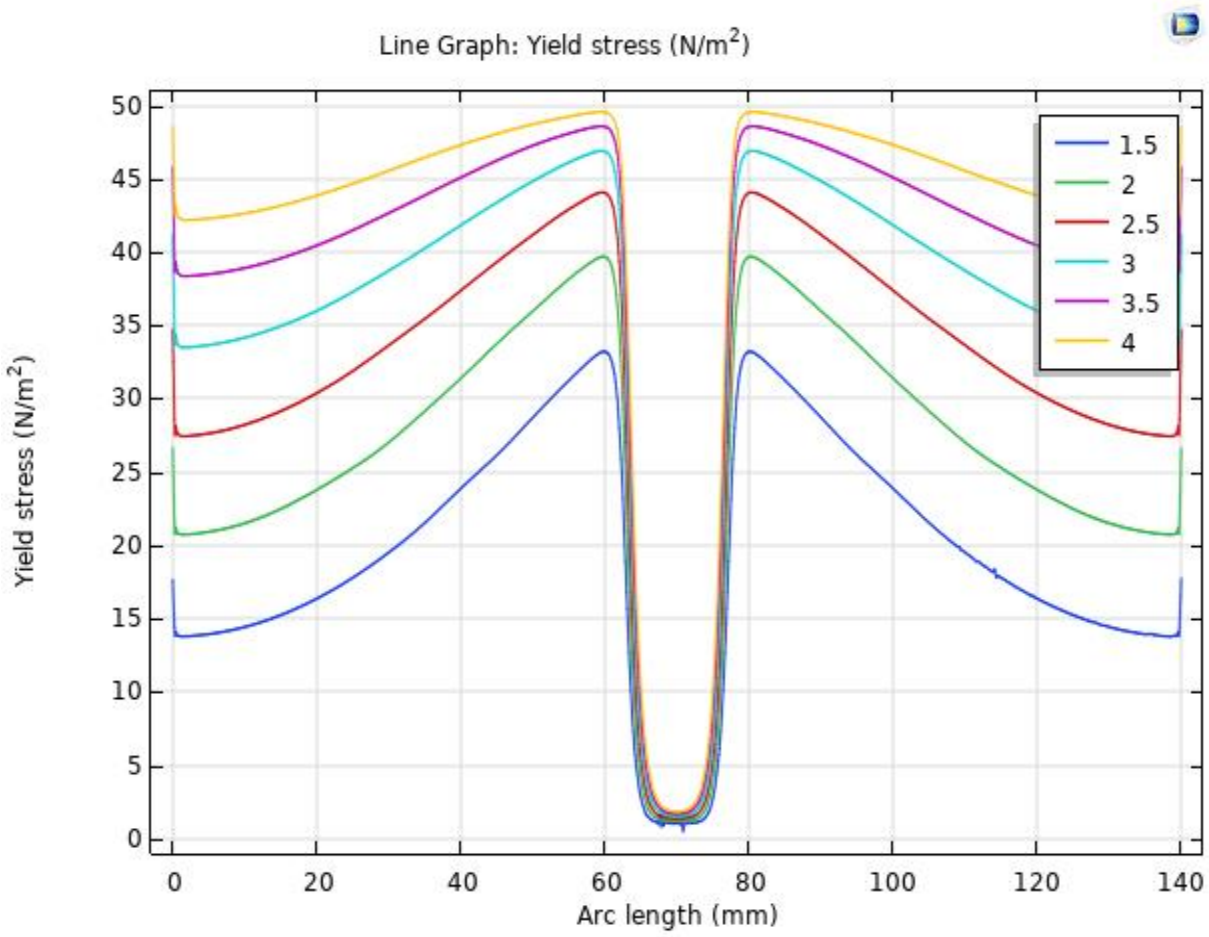

Fig.4.27 Yield stress for different currents with a gap size of 1.5mm

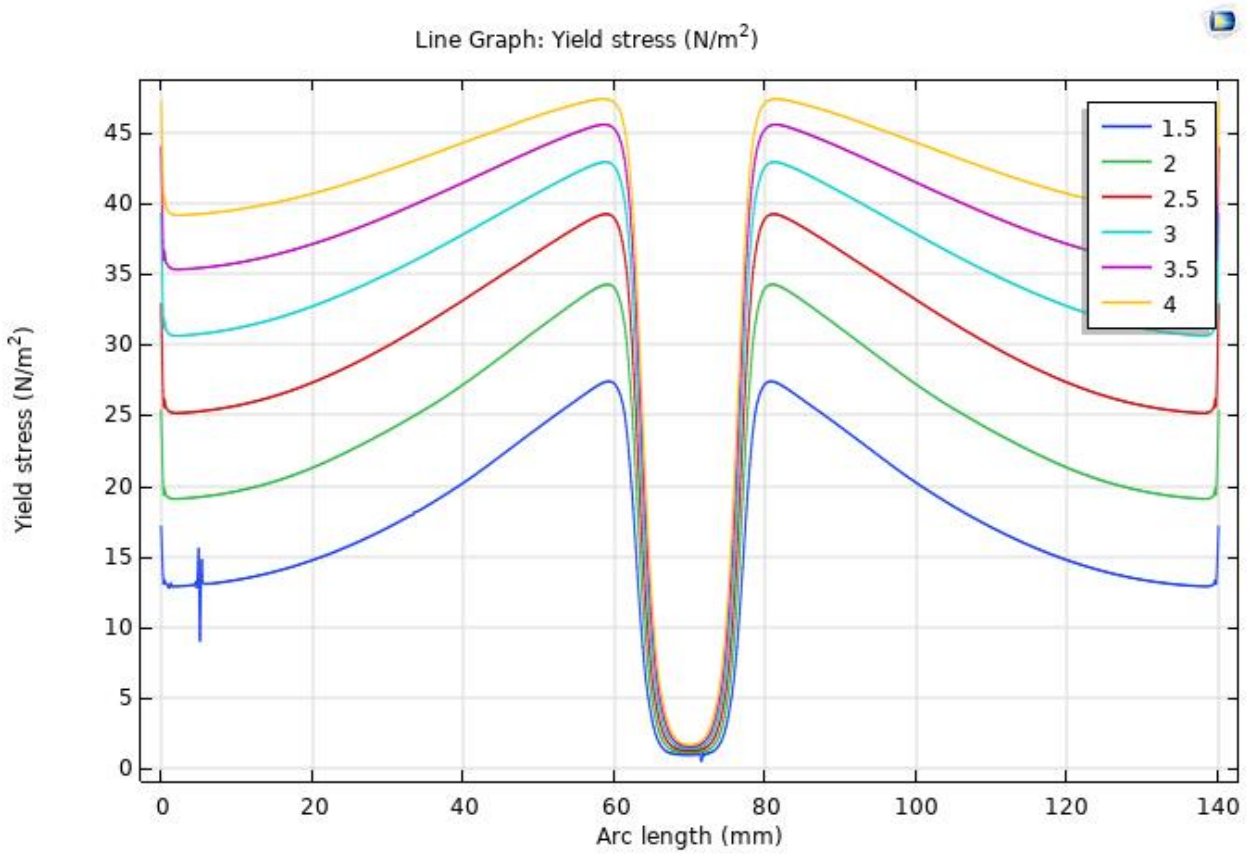

Fig.4.28 Yield stress for different currents with a gap size of 2mm

Comparing the yield stress for the gap sizes 1mm, 1.5mm and 2mm with coil turns number 400 for the currents 1.5A, 2A, 2.5A, 3A, 3.5A and 4A the yield stress decreases with the increase in gap size of MR fluid flow region. Considering the current 1.5A for the gap size 1mm the maximum yield stress is 40 N/m^2, for 1.5mm gap size the maximum yield stress is 33 N/m^2 and for 2mm gap size the maximum yield stress is 27 N/m^2. The percentage of decrease of yield stress from 1mm gap to 2mm is 33%. The yield stress decreases as the damping gap increases due to the decrease in magnetic flux density. This decrease in yield stress affects the decrease in the dynamic viscosity.

CHAPTER 5

CONCLUSION

Magnetostatic analysis is done on the MR damper in COMSOL Multiphysics software for a 2D Axisymmetric model. The analysis is done for the magnetic flux density, yield stress and dynamic viscosity for the number of turns in coil 300,400,500 and 600 and the current given for each set of coils are 1.5A, 2A, 2.5A, 3A, 3.5A and 4A. The influence of gap size for the MR fluid flow region is evaluated. The gap sizes given for the proposed model are 1mm, 1.5mm and 2mm.

The magnetic flux density analysis shows that as the increase in current the magnetic flux density at MR fluid also increases. The increase in percentage for the magnetic flux density for the increase in current with respect to the number of turns in coil are: -

1. For 300 turns of coils the percentage increase of magnetic flux density from 1.5A to 4A current is 73%.
2. For 400 turns of coils the percentage increase of magnetic flux density from 1.5A to 4A current is 77%.
3. For 500 turns of coils the percentage increase of magnetic flux density from 1.5A to 4A current is 81%.
4. For 600 turns of coils the percentage increase of magnetic flux density from 1.5A to 4A current is 84%.

The magnetic flux density analysis also shows that as the number of turns in coil increases the magnetic flux density also increases. The increase in percentage for the magnetic flux density for the increase in number of turns for the coil with respect to the current are: -

1. For the current 1.5A with increase in the coil turns number from 300 to 600 is 46%.
2. For the current 4A with increase in the coil turns number from 300 to 600 is 55%.

Comparing the dynamic viscosities for different currents for different number of turns of coils the inference obtained is when the coil turns number increases the dynamic viscosity also increases. Maximum dynamic viscosity is near to the effective magnetic poles. The increase in percentage for the dynamic viscosity from coil turns number300 to 600 for the current 1.5A is 33% and for the current 4A is 20%.

Comparing the yield stresses for different currents for different coil turns number as the coil turns number increases the yield stress also increases. Yield stress increases with the increase in current. The increase in yield stress is influenced in the increase the dynamic viscosity of the MR fluid.

The influence of gap size affecting is analyzed for the model by varying the MR fluid gap from 1mm to 1.5mm and 2mm with the number of turns of coils as 400 for magnetic flux density, yield stress and dynamic viscosity.

The magnetic flux density is reviewed and inference is as the magnetic flux density decreases as the gap is increased for the same current. There is a decrease of 5% in magnetic flux density for 1.5A current for the change in gap from 1mm to 1.5mm, A decrease of 4% in magnetic flux density for 1.5A current for the change in gap from 1.5mm to 2mm and a decrease of 8% in magnetic flux density for 1.5A current for the change in gap from 1mm to 2mm.

Comparing the dynamic viscosities for the gap sizes 1mm, 1.5mm and 2mm with coil turns number400 for the currents 1.5A, 2A, 2.5A, 3A, 3.5A and 4A the dynamic viscosity decreases with the increase in gap size of MR fluid flow region. The damping effect decreases as the decrease in viscosity and as there by there is a need for an optimum gap for an effective damping considering the damping force needed to accommodate by the MR damper.

The yield stress decreases as the damping gap increases due to the decrease in the magnetic flux density. This decrease in the yield stress affects the decrease in the dynamic viscosity.

REFERENCES

1. **Wang, F, Qian, Z, Yan, Z, Yuan, C, Zhang, W** (2020). A Novel Resilient Robot: Kinematic Analysis and Experimentation.
2. **Zhang, T, Zhang,W, Gupta, M** (2017). Resilient Robots: Concept, Review, and Future Directions. Robotics 6, 22.
3. **Spencer B S Jr, Dyke S, SainMand Carlson J** (1997). Phenomenological model of a magnetorheological damper J. Eng. Mech. 123 230–8.
4. **B. P. Ronge, S. R. Kajale, P. M. Pawar** "Theoretical and Experimental analysis of MR fluid dampers: Design and Performance analysis", LAP launcher academic publication, ISBN 978-3-8454-7757-2, German, Paperback, 192 pages.
5. **Parlak, Z, Engin, T, Çallı, ˙I** (2012). Optimal design of MR damper via finite element analyses of fluid dynamic and magnetic field. Mechatronics 22, 890–903.
6. **A. Sternberg, R. Zemp, J.C. de la Llera** (2009). Multiphysics behavior of a magnetorheological damper and experimental validation, Eng. Struct. 69 194–205.
7. **ZhangHH, LiaoCR, ChenWMand Huang S L** (2006). A magnetic design method of MRfluid dampers and FEManalysis on magnetic saturation J. Intell. Mater. Syst. Struct. 17 813–8.
8. **Yazid, S.A. Mazlan, T. Kikuchi, H. Zamzuri, F. Imaduddin** (2013). Design of magnetorheological damper with a combination of shear and squeeze modes, Mater. Des. 1980–2015 (54) 87–95.
9. **Khan MA, Suresh A and Ramaiah NS** (2012). Investigation on the performance of MR damper with various piston configurations. International Journal of Scientific and Research Publications 2 1–7.

10. **Md. Sadak Ali Khan, A.S.; Seetha Ramaiah, N. Seetha Ramaiah** (2012). Analysis of Magneto Rheological Fluid Damper with Various Piston Profiles. Int. J. Eng. Adv. Technol.
11. **Yang, Xu, Guo, Xu, Zhang, J** (2020). Internal magnetic field tests and magnetic field coupling model of a three-coil magnetorheological damper. J. Intell. Mater. Syst. Struct. 31, 2179–2195.
12. **Golinelli, N, Spaggiari, A** (2017). Experimental validation of a novel magnetorheological damper with an internal pressure control. J. Intell. Mater. Syst. Struct. 28, 2489–2499.
13. **Ashwani Kumar, S.K. Mangal** (2014). Finite element analysis of magneto-rheological damper. Asian J. Eng. Appl. Technol. (AJEAT).
14. **Ferdaus, Rashid, Hasan, Rahman** (2014) Optimal design of magneto-rheological damper comparing different configurations by finite element analysis J. Mech. Sci. Technol. 28 3667–77
15. **K. Hemanth, A. Ganesha, H. Kumar, K.V, Gangadharan** (2014). Analysis of MR damper based on Finite Element Approach, Appl. Mech. Mater. 592–594 2006–2010.
16. **Case DA, Taheri B and Richer E** (2013) Multiphysics modeling of magnetorheological dampers The International Journal of Multiphysics7 61–76.
17. **Guoliang Hu, Lifan Wu, Yingjun Deng, Lifan Yu and Bin Luo** (2021). Damping Performance Analysis of Magnetorheological Damper Based on Multiphysics Coupling.
18. **Liankang Wei, Hongzhan Lv, Kehang Yang, Weiguang Ma, Junzheng Wang and Wenjun ZhangA** (2021). Comprehensive Study on the Optimal Design of Magnetorheological Dampers for Improved Damping Capacity and Dynamical Adjustability.

19. **Raju Ahamed, Muhammad Mahbubur Rashid, Md Meftahul Ferdaus and Hazlina Md. Yusof** (2016). Design and modeling of energy generated magneto rheological damper.
20. **W.A. Bullough, D.J. Ellam, A.P. Wong, R.C. Tozer** (2007). Computational fluid dynamics in the flow of ERF/MRF in control devices and of oil through piezo-hydraulic valves.
21. **Zekeriya Parlak, Tahsin Engin, Ismail Çallı** (2012). Optimal design of MR damper via finite element analyses of fluid dynamic and magnetic field.
22. **S. Vivekananda Sharma a, G. Hemalatha a, K. Ramadevi** (2021). Analysis of magnetic field-strength of multiple coiled MR-damper using COMSOL Multiphysics.
23. **COMSOL Co., L.** (2019). CFD Module User's Guide-Theory for the Single-Phase Flow Interface, 5.5th ed.; COMSOL Co., Ltd.: Burlington, NJ, USA, pp. 139–141.